

Ion Coulomb crystals: Thermodynamics, Quantum dynamics and Simulators

Giovanna Morigi
Universität des Saarlandes
Theoretische Physik

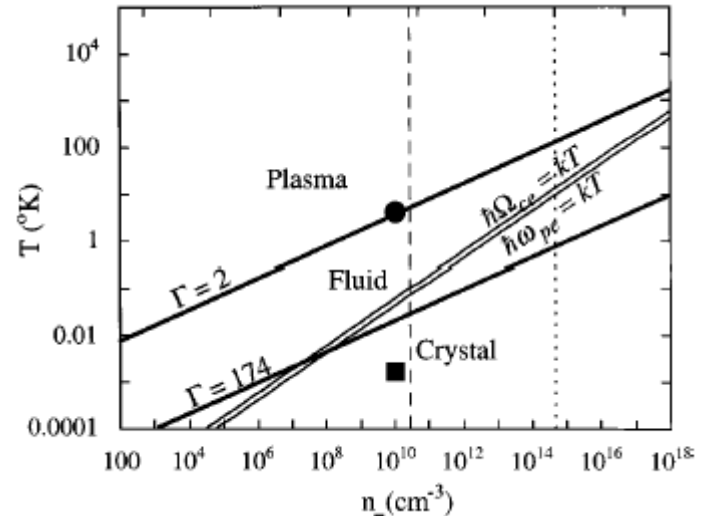
One-component plasma (homogeneous system, 3D)

Coupling parameter: $\Gamma = e^2 / akT$

$a = (3/4\pi n)^{1/3}$ Wigner-Seitz radius

Strong correlations: $\Gamma \gg 1$

Crystallization (transition to spatial order): $\Gamma = 174$



One-component plasmas in atomic physics

Bragg Diffraction from Crystallized Ion Plasmas

W. M. Itano,* J. J. Bollinger, J. N. Tan,† B. Jelenković,‡
X.-P. Huang, D. J. Wineland

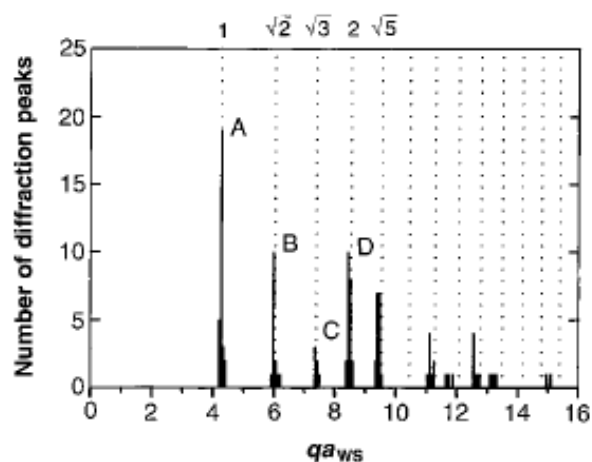
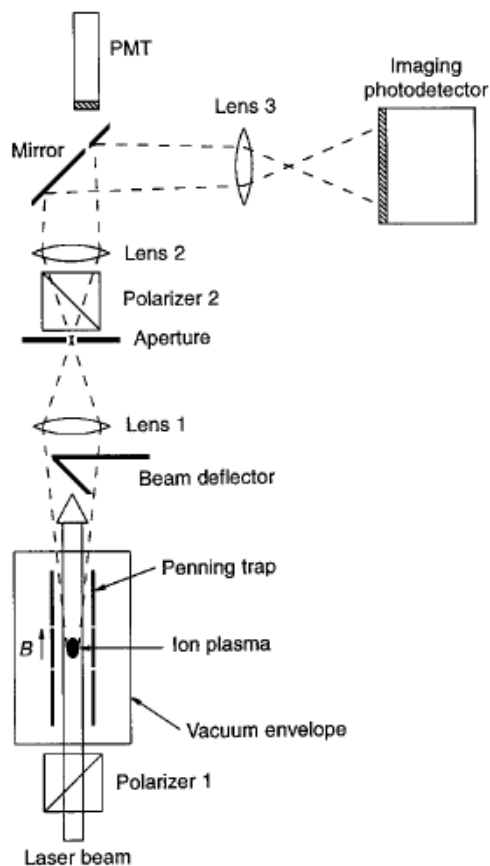


Fig. 3. Histogram representing the numbers of peaks (not intensities) observed as a function of qa_{ws} , where $\mathbf{q} = \mathbf{k}_s - \mathbf{k}_i$ is the difference between the incident (\mathbf{k}_i) and scattered (\mathbf{k}_s) photon wave vectors. We analyzed 30 Bragg diffraction patterns from two approximately spherical plasmas having 270,000 and 470,000 ions. The dotted lines show the expected peak positions, normalized to the center of gravity of the peak at A ($\{110\}$ Bragg reflections).

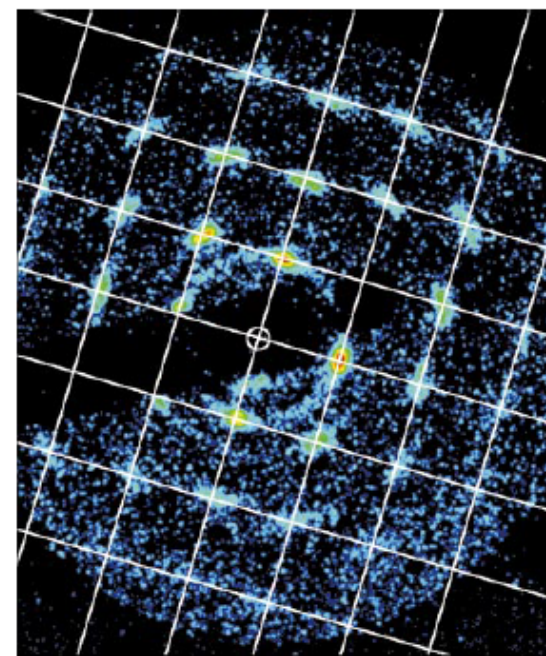


Fig. 4. Time-resolved Bragg diffraction pattern of the same plasma as in Fig. 2. Here and in Figs. 5 and 6 the small open circle marks the position of the undeflected laser beam. A bcc lattice, aligned along a $\langle 100 \rangle$ axis, would generate a spot at each intersection of the grid lines overlaid on the image. The grid spacing corresponds to an angular deviation of 2.54×10^{-2} rad. Here, $\omega_r = 2\pi \times 125.6$ kHz, $n_0 = 3.83 \times 10^9$ cm $^{-3}$, $N = 5 \times 10^5$, $\alpha = 0.98$, and $2r_0 = 1.36$ mm.

Coulomb gas in atomic physics

- 1) Gas of ionized atoms:
usually singly-ionized alkali-earth metals
(e.g. Berillium, Calcium, Magnesium).
Radiation is absorbed and emitted in the visible.

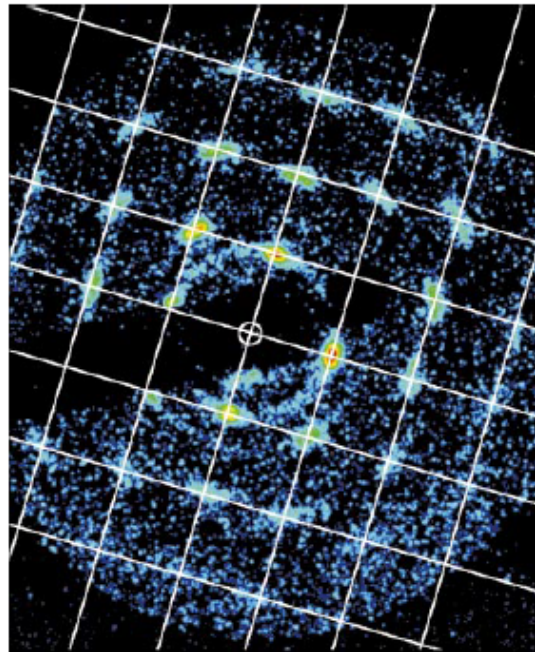
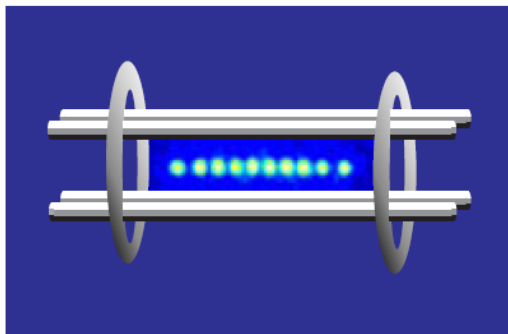


Fig. 4. Time-resolved Bragg diffraction pattern of the same plasma as in Fig. 2. Here and in Figs. 5

Coulomb gas in atomic physics

1) Gas of ionized atoms:
usually singly-ionized alkali-earth metals.
Radiation is absorbed and emitted in the visible.

2) Confinement by external potentials:
Paul (radiofrequency) or Penning traps.



Innsbruck Ion trap

Linear Paul trap:

$$\Phi_0 = U_{\text{dc}} + V_{\text{ac}} \cos(\Omega_{\text{rf}} t)$$

Effective harmonic force $\mathbf{F} \propto -\mathbf{r}$

Possibility to control the number of ions and the shape of the cloud

Coulomb gas in atomic physics

- 1) Gas of ionized atoms:
usually singly-ionized alkali-earth metals.
Radiation is absorbed and emitted in the visible.
- 2) Confinement by external potentials:
Paul (radiofrequency) or Penning traps.
- 3) Crystallization:
Low thermal energies are achieved by laser cooling.
Cooling down to *few microKelvin*.

Crystals of ions in traps: Applications

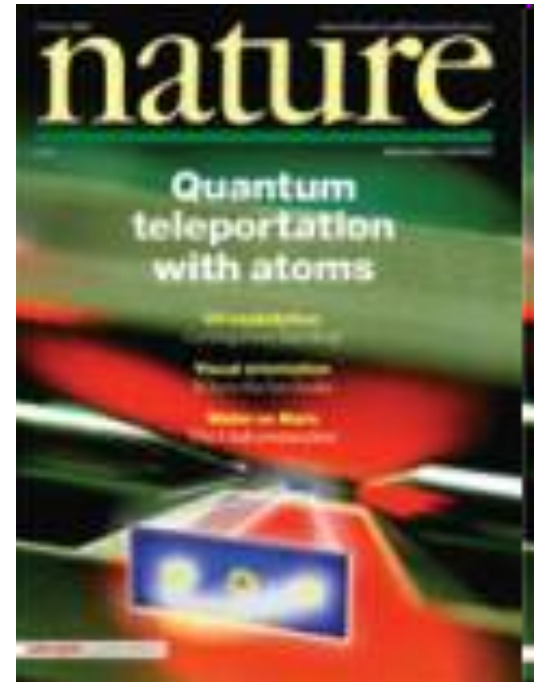
High-precision measurements

Simulation of astrophysical systems

Ultracold chemistry

Quantum-based technologies

Quantum simulators, quantum metrology,
Quantum computing.



Aarhus, Berkeley, Boulder, Freiburg, Erlangen, Innsbruck, London, Mainz, Marseille, Michigan, München, Oxford, Paris, PTB, Saarbrücken, Siegen, Sussex,

Cirac, Zoller, Retzker, Plenio, Altman, Porras, Solano, Duan, ...

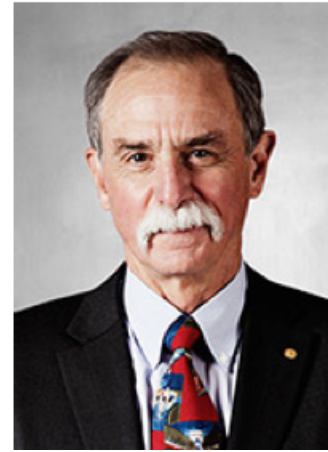
Trapped ions and Nobel Foundation



Dehmelt (1989)



Paul (1989)



Wineland (2012)

The Nobel Prize in Physics 1989 was divided, one half awarded to Norman F. Ramsey *"for the invention of the separated oscillatory fields method and its use in the hydrogen maser and other atomic clocks"*, the other half jointly to Hans G. Dehmelt and Wolfgang Paul *"for the development of the ion trap technique"*.

The Nobel Prize in Physics 2012 was awarded jointly to Serge Haroche and David J. Wineland *"for groundbreaking experimental methods that enable measuring and manipulation of individual quantum systems"*

And also: **Ramsey (1989), Chu, Cohen-Tannoudji, Phillips (1997), Haroche (2012)**

Low dimensional structures

VOLUME 68, NUMBER 13

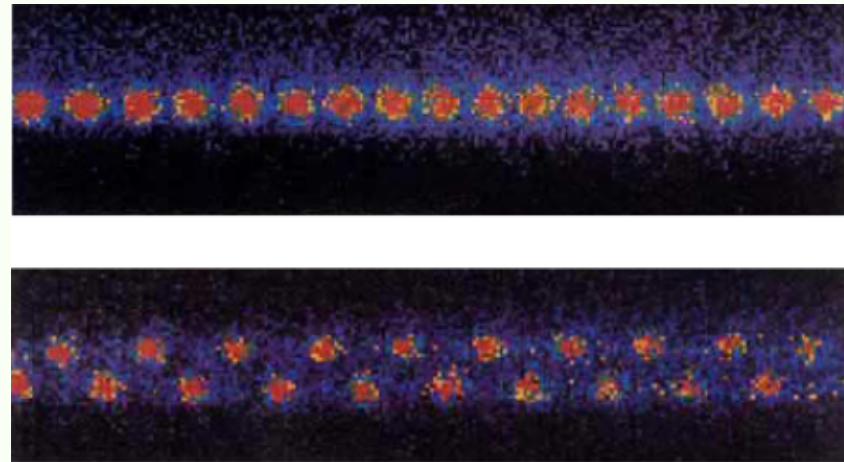
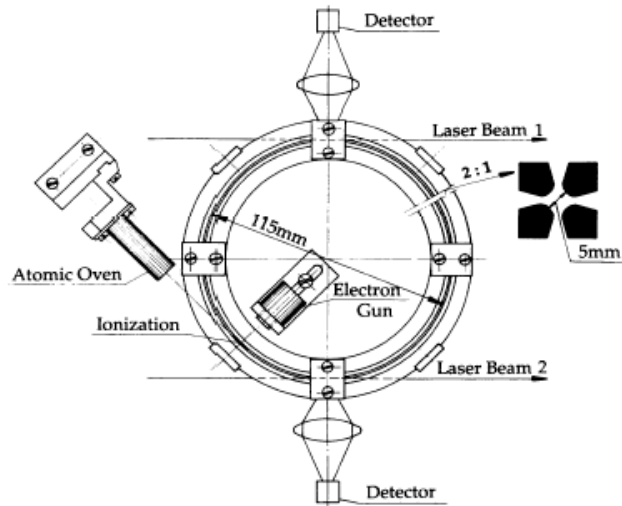
PHYSICAL REVIEW LETTERS

30 MARCH 1992

Observation of Ordered Structures of Laser-Cooled Ions in a Quadrupole Storage Ring

I. Waki,^(a) S. Kassner, G. Birkel, and H. Walther

Max-Planck-Institut für Quantenoptik, D-8046 Garching bei München, Federal Republic of Germany
(Received 11 September 1991; revised manuscript received 16 December 1991)



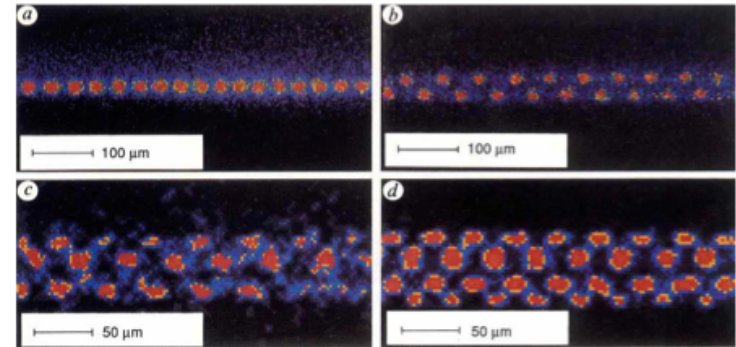
[Birkel et al., Nature 357, 310 (1992)]

Phase diagram

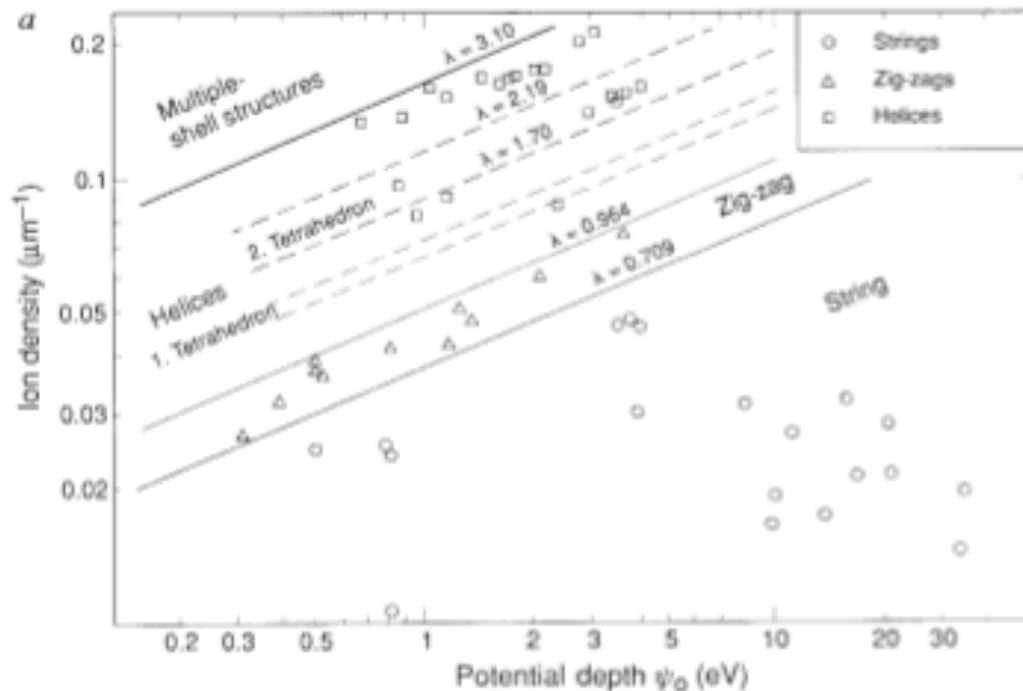
Multiple-shell structures of laser-cooled $^{24}\text{Mg}^+$ ions in a quadrupole storage ring

G. Birkl, S. Kassner & H. Walther

Max-Planck-Institut für Quantenoptik, Garching bei München, Germany



Nature 357, 310 (1992)



Outline

1. Thermodynamics of ion chains

- the linear-zigzag instability, classical PT
- the linear-zigzag instability, quantum PT

2. Dynamics of ion chains across the instability

- Classical quenches
- Quantum quenches

3. Outlook. Topological Structural Transitions

Thermodynamics of ion chains

The ion chain

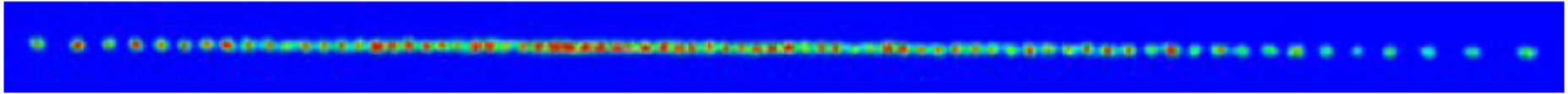
In textbooks (Ashcroft and Mermin):



Periodic distribution: Bloch theorem

Long-range interaction (Coulomb): no sound velocity

The ion chain in a linear trap



(M. Drewsen and coworkers, Aarhus)

$$H = \sum_{j=1}^N \frac{\mathbf{p}_j^2}{2m} + \frac{1}{2} m \left(\nu^2 x_j^2 + \nu_t^2 (y_j^2 + z_j^2) \right) + \frac{1}{2} \sum_{j=1}^N \sum_{i \neq j} \frac{Q^2}{r_{i,j}}$$

$\nu \ll \nu_t$ 1D structure (ion chain)

Inhomogeneous distribution: NO Bloch theorem

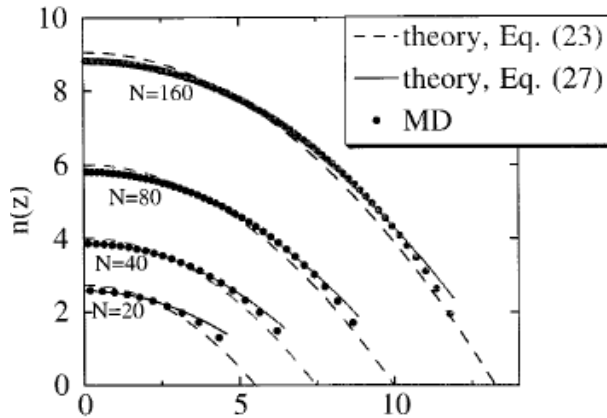
Long-range interaction:

perturbation theory with Bloch waves does not converge

Charge density at equilibrium

$$m\nu^2 x_i^{(0)} = - \sum_{j>i} \frac{Q^2}{(x_j^{(0)} - x_i^{(0)})^2} + \sum_{j<i} \frac{Q^2}{(x_i^{(0)} - x_j^{(0)})^2}$$

Continuum limit: mean field description for 1D



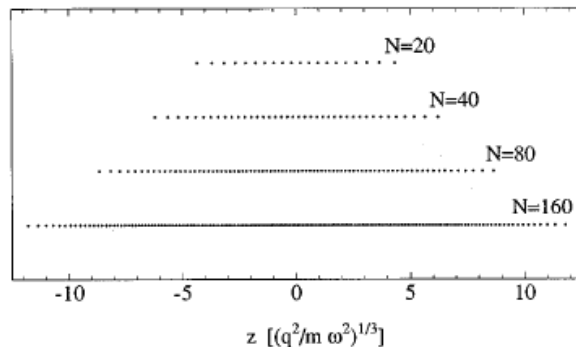
Linear density:

$$n_L(x) = \frac{3N}{4L} \left(1 - \frac{x^2}{L^2} \right)$$

Length of the chain:

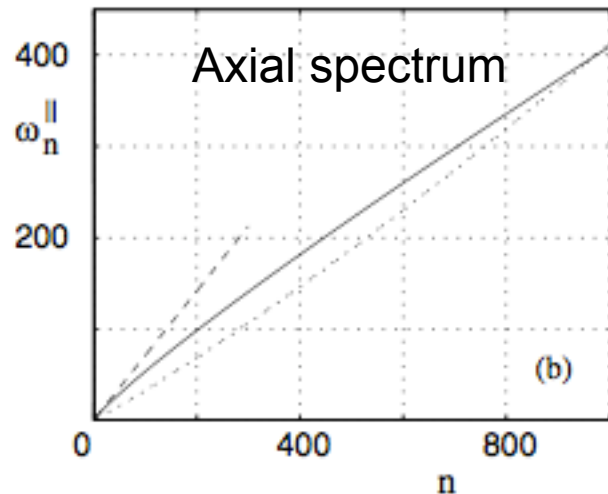
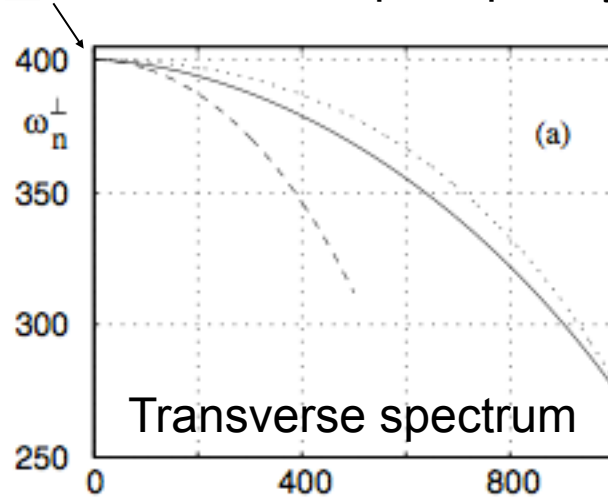
$$L(N)^3 = 3 \left(\frac{Q^2}{m\nu^2} \right) N \log N$$

at leading order in $1/\log N$



Spectra of excitations

ν_t Transverse trap frequency



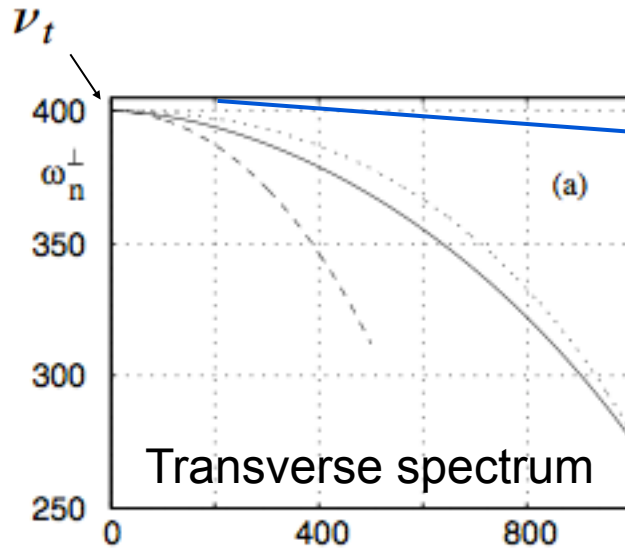
$$\ddot{q}_i = -\nu^2 q_i - \sum_{j \neq i} \frac{K_{i,j}}{m} (q_i - q_j),$$

$$\ddot{y}_i = -\nu_t^2 y_i + \frac{1}{2} \sum_{j \neq i} \frac{K_{i,j}}{m} (y_i - y_j),$$

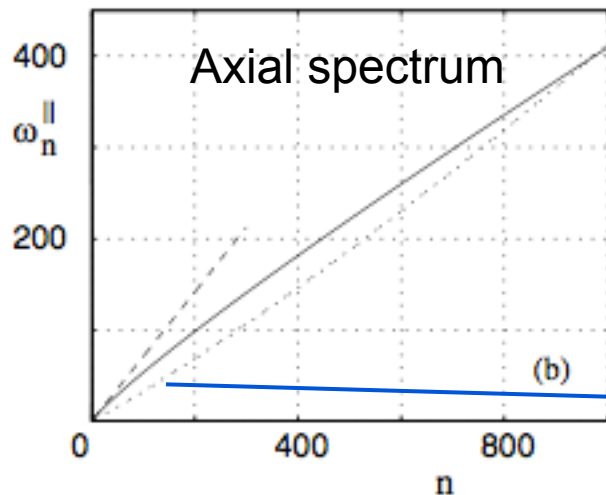
$$\ddot{z}_i = -\nu_t^2 z_i + \frac{1}{2} \sum_{j \neq i} \frac{K_{i,j}}{m} (z_i - z_j),$$

$$K_{ij} = \frac{2Q^2}{|x_i^{(0)} - x_j^{(0)}|^3}.$$

Spectra of excitations

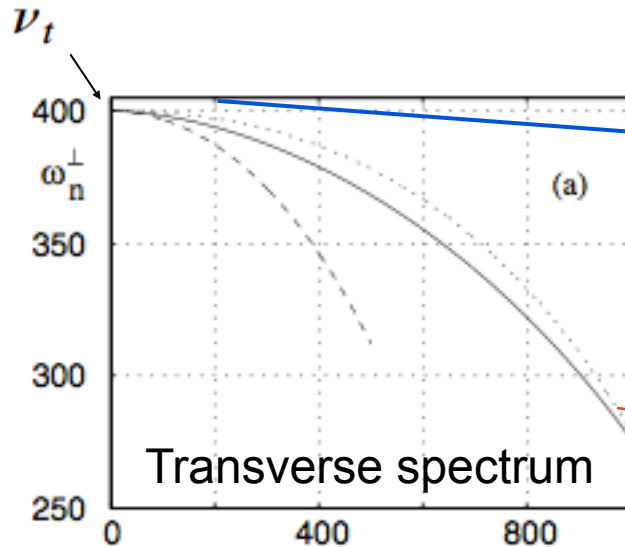


Long wavelength modes:
Jacobi polynomials



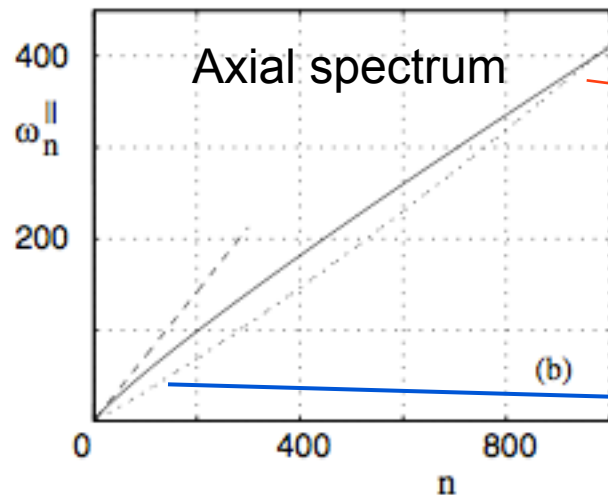
Long wavelength modes:
Jacobi polynomials

Spectra of excitations



Long wavelength modes:
Jacobi polynomials

Short wavelength modes:
Phononic waves



Short wavelength modes:
Phononic waves

Long wavelength modes:
Jacobi polynomials

Statistical Mechanics

Quantization of the vibrations

$$\hat{H}_n = \sum_{n=1}^N \hbar \omega_n^{\parallel} \hat{N}_n^{\parallel} + \sum_{n=1}^N \hbar \omega_n^{\perp} (\hat{N}_{n,y}^{\perp} + \hat{N}_{n,z}^{\perp})$$

Canonical ensemble

$$\rho = \frac{1}{Z} \exp(-\beta H)$$

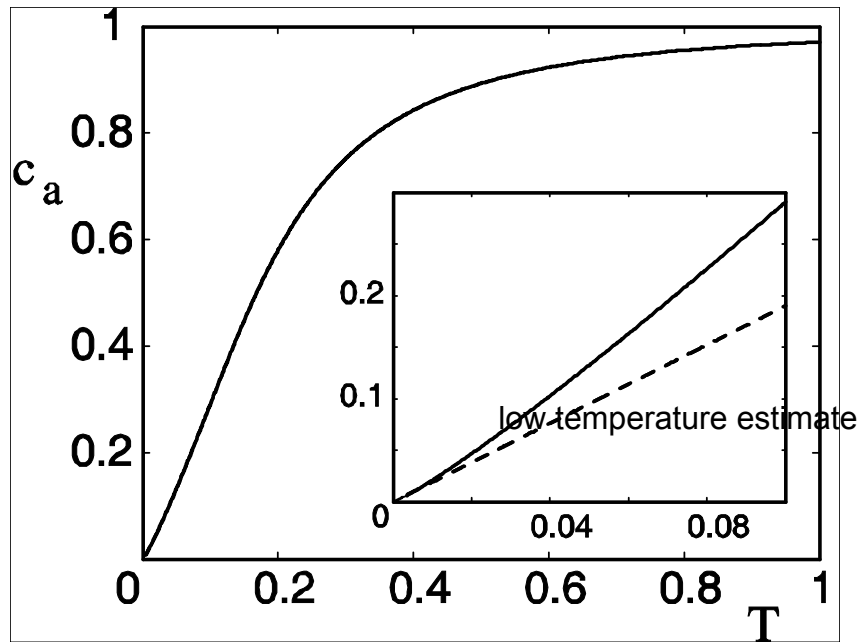
$$F = -k_B T \log Z$$

One-dimensional behaviour: $k_B T \ll \hbar \omega_{\min}^{\perp}$

Thermodynamic limit: $\nu \sim \sqrt{\log N}/N$ as $N \rightarrow \infty$

Density in the center $n(0) = \frac{3}{4} \frac{N}{L}$ fixed

Specific Heat



Non extensive behaviour at low temperatures in the thermodynamic limit:

$$c_a \propto 1 / \sqrt{\ln N}$$

- Due to long-range Coulomb interaction
- It is a quantum effect (at high-T Dulong-Petit holds)

Ion chains are thermal reservoirs?

- In the *harmonic* chain the dynamics is integrable

JOURNAL OF MATHEMATICAL PHYSICS

VOLUME 6, NUMBER 4

APRIL 1965

Statistical Mechanics of Assemblies of Coupled Oscillators*

G. W. FORD†

Department of Physics, University of Michigan, Ann Arbor, Michigan

M. KAC

The Rockefeller Institute, New York, New York

AND

P. MAZUR

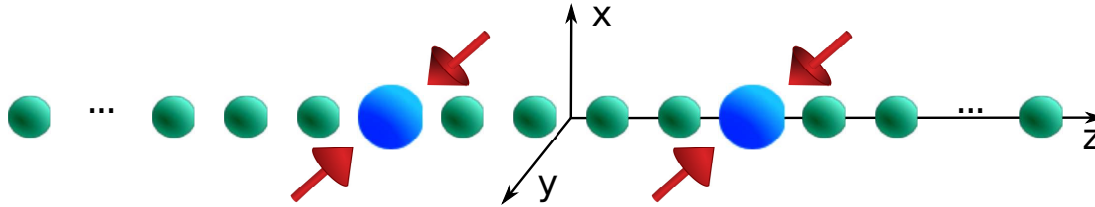
Lorentz Institute for Theoretical Physics, Leiden, The Netherlands

(Received 25 September 1964)

It is shown that a system of coupled harmonic oscillators can be made a model of a heat bath. Thus a particle coupled harmonically to the bath and by an arbitrary force to a fixed center will (in an appropriate limit) exhibit Brownian motion. Both classical and quantum mechanical treatments are given.

- The rest of the chain acts as a bath for a single ion (when thermalization rate is faster than recurrence)

Ion chain as quantum reservoir



Langevin equation:

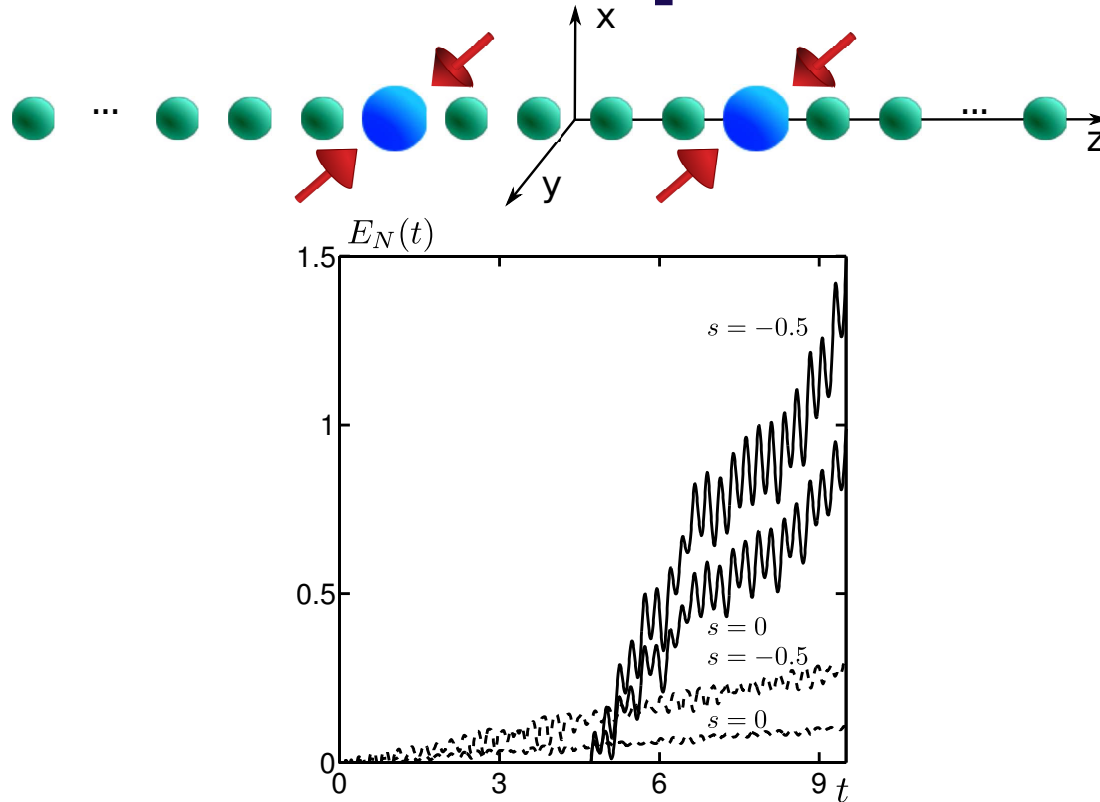
$$\frac{d^2 X_{\pm}}{dt^2} + \int_0^t \Gamma_{\pm}(t-t') \frac{dX_{\pm}}{dt'} dt' + (1 - \Gamma_{\pm}(0)) X_{\pm}(t) = F_{\pm}(t) - \Gamma_{\pm}(t) X_{\pm}(0)$$

damping kernel

Spectral density (Fourier transform of the damping kernel)

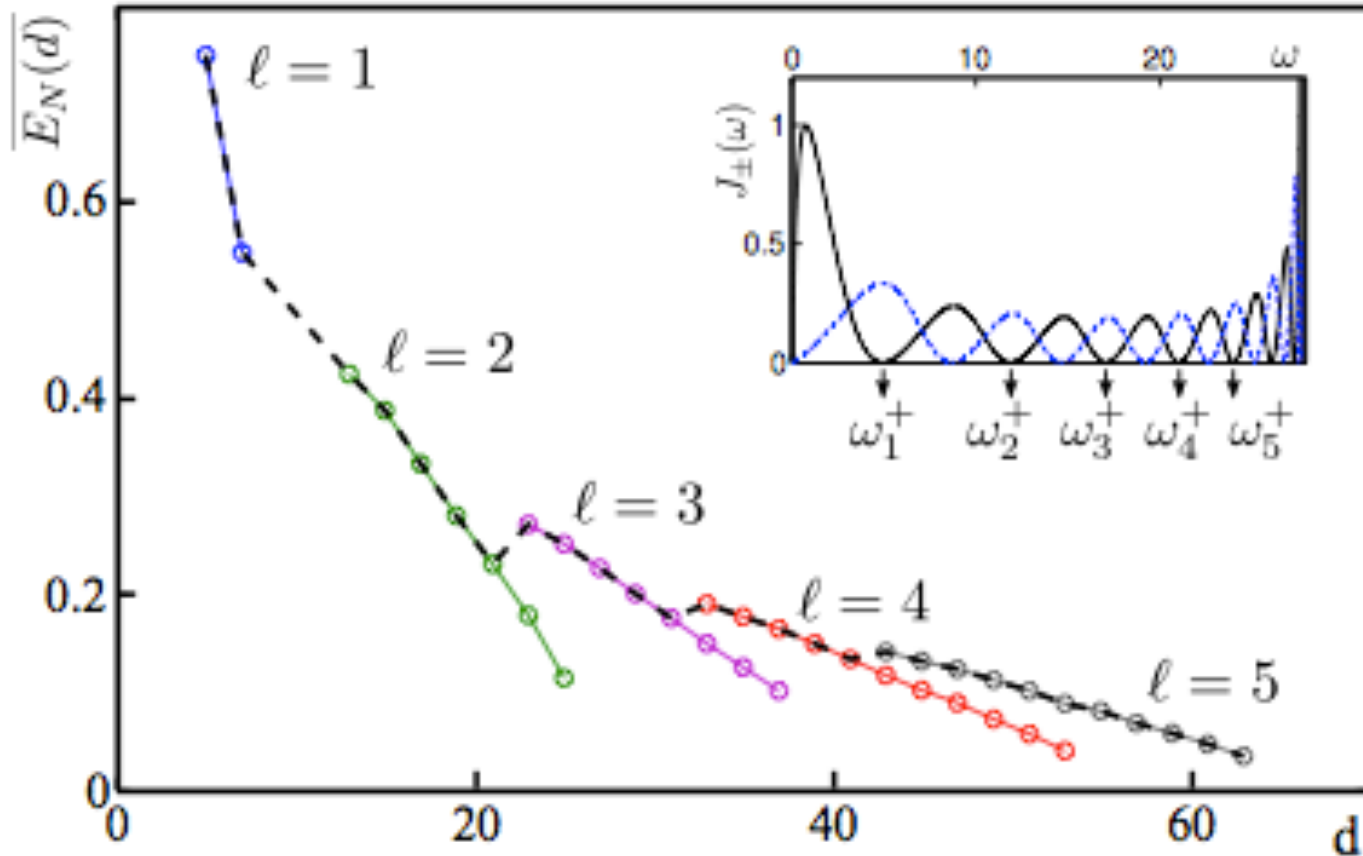
$$J_{\pm}(\omega) = \omega \int_0^{\infty} \Gamma_{\pm}(t) \cos(\omega t) dt$$

Entangle two distant ions after a quench



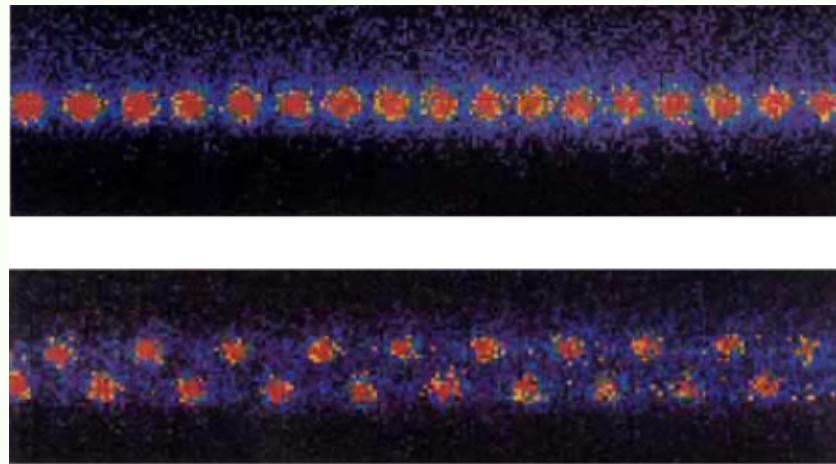
distance $d=5a$, chain of 50 ions in a thermal state
(ions: Calcium, impurity defects: Indium).

Scaling with the distance



linear decay with the distance

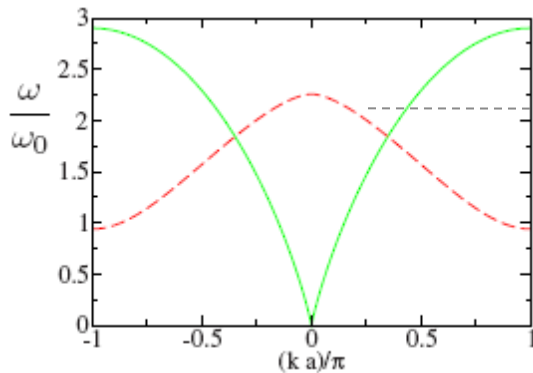
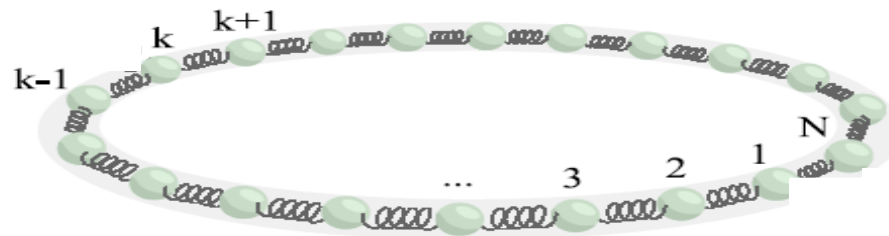
Linear-zigzag instability



[Birkel et al., Nature 357, 310 (1992)]

Preamble: Ring

No axial confinement: periodic distribution
 Modes are phononic waves with quasimomentum k in BZ



$$\nu_t \quad \omega_{\perp}(k)^2 = \nu_t^2 - 2 \left(\frac{2Q^2}{ma^3} \right) \sum_{j=1}^N \frac{1}{j^3} \sin^2 \frac{jka}{2}$$

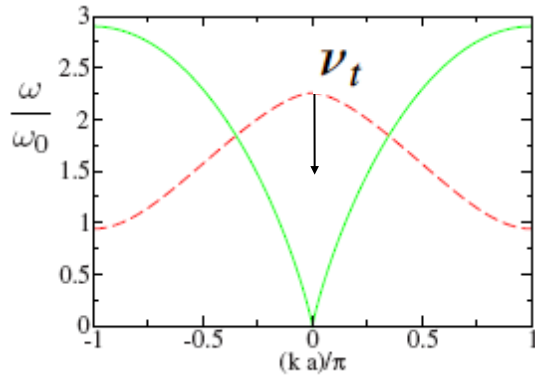
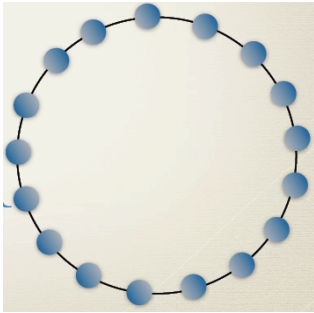
Instability: $\omega_{\perp}^2 < 0$

Critical value: $\nu_t^{(c)2} = 2 \left(\frac{2Q^2}{ma^3} \right) \sum_{j=1}^N \frac{1}{j^3} \sin^2 \frac{j\pi}{2} \rightarrow \frac{Q^2}{ma^3} \frac{7}{2} \zeta(3)$

Transition chain-zigzag

decrease transverse confinement ν_t

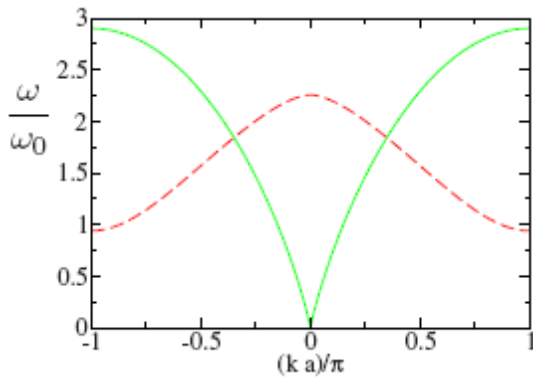
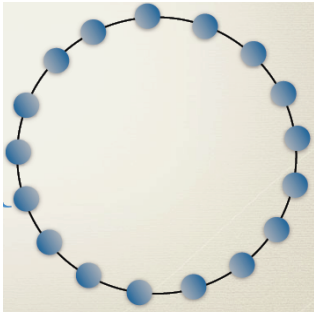
Linear chain



Transition chain-zigzag

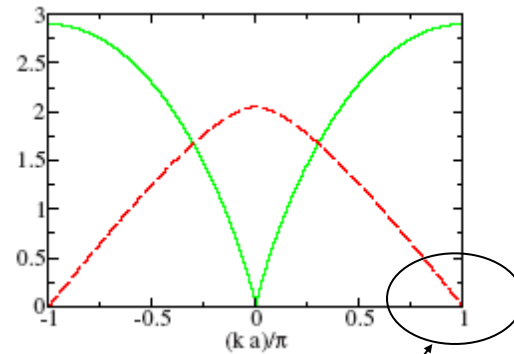
decrease transverse confinement

Linear chain

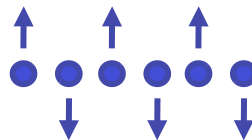


Transition point

$$v_t^{(c)}$$



Zigzag mode

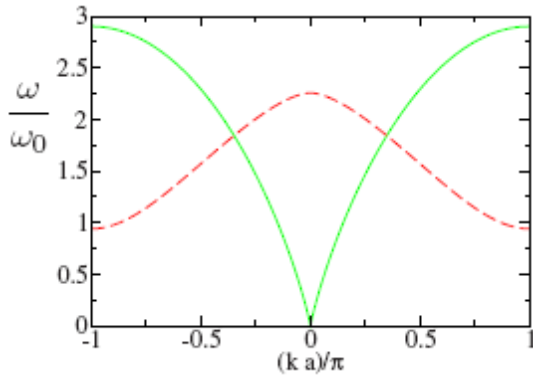


Transition chain-zigzag

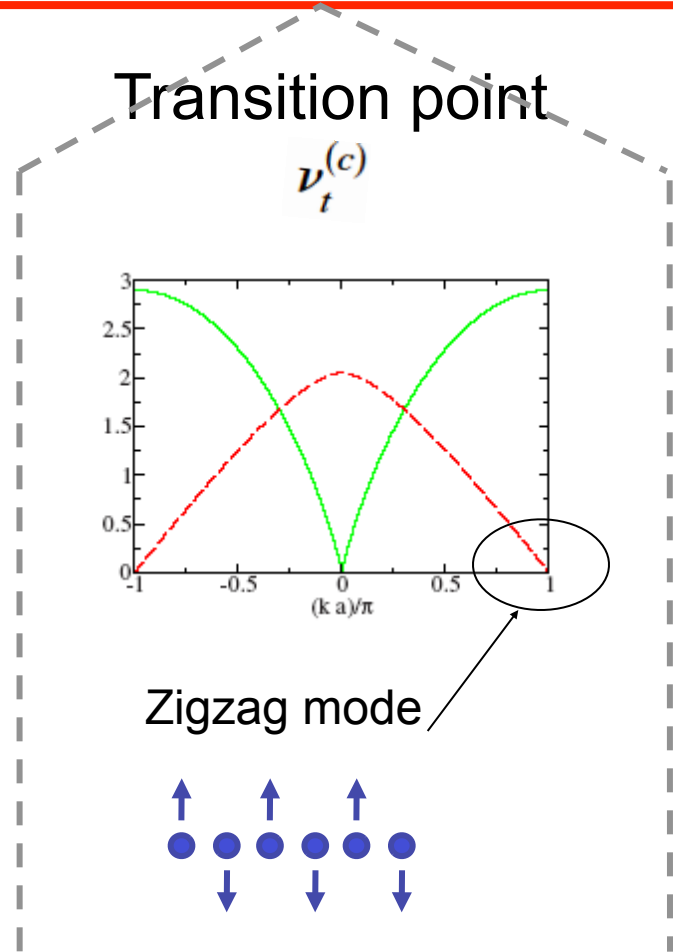
decrease transverse confinement



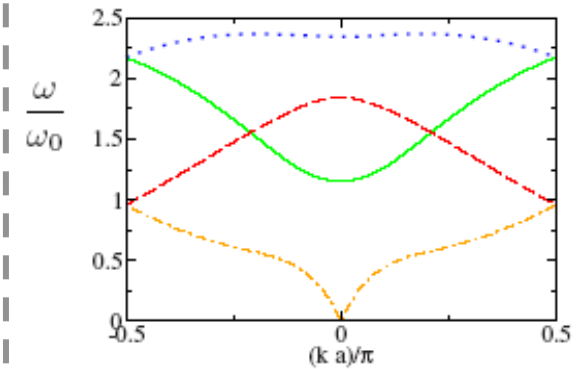
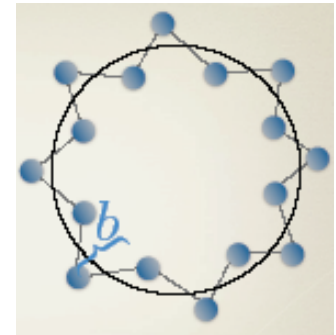
Linear chain



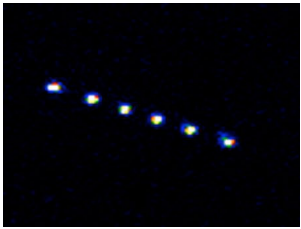
Transition point



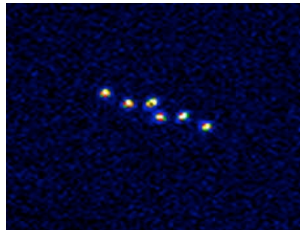
Zigzag



Chain to Zig-Zag: second-order phase transition?

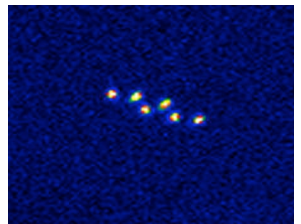


Symmetry breaking: line to plane



Order parameter: Distance from the axis

Control field: Transverse frequency



Soft mode: Zigzag mode

Potential at the instability

Ansatz: the zigzag mode is the soft mode.

Expand the potential at 4th order in plane waves
Study new minima as a function of transverse freq.

$$V_{\text{eff}} = \frac{m}{2} \beta_0 \left[\underbrace{\Psi_0^{y^2} + \Psi_0^{z^2}}_{\text{zigzag mode}} \right] + \frac{m}{2} \sum_{\delta k > 0} \beta_{\delta k} \sum_{\sigma=y,z} \left[\Psi_{\delta k}^{\sigma(+)^2} + \Psi_{\delta k}^{\sigma(-)^2} \right] + V_0^{(4)}$$

other modes

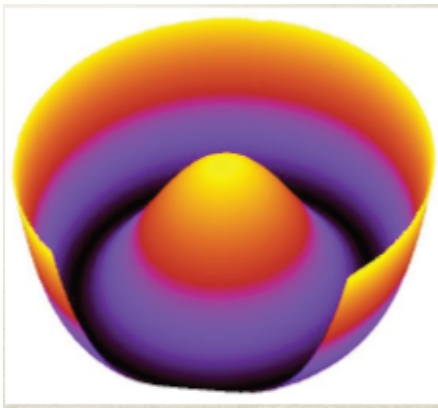
$$\beta(k) = v_t^2 - 2 \left(\frac{2Q^2}{ma^3} \right) \sum_{j=1}^N \frac{1}{j^3} \sin^2 \frac{jka}{2}$$

Check for $\frac{\partial^2 V_{\text{eff}}}{\partial \Psi_{\delta k}^{y(\pm)} \partial \Psi_{\delta k}^{z(\mp)}} > 0$

Potential of the zigzag mode

Derivation of the effective potential for the zigzag mode:

$$V^{\text{soft}} = \mathcal{V}[(\Psi_0^y)^2 + (\Psi_0^z)^2] + A[(\Psi_0^y)^2 + (\Psi_0^z)^2]^2$$



$$\mathcal{V} = \frac{m}{2} \beta_0 = \frac{1}{2} m (v_t^2 - v_t^{(c)2})$$
$$A = \frac{3}{2} \frac{31}{32} \zeta(5) \frac{Q^2}{a^5}$$

The other modes are stably trapped by a harmonic potential
(microscopic derivation of Landau model)

Summary:

classical phase transition

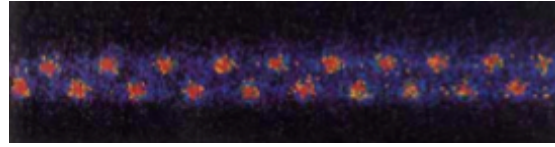
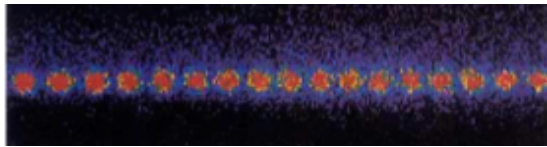
- Microscopic derivation of the Landau model.
- Second-order phase transition.
- Critical exponents of Landau model.
- Soft mode: zigzag mode.

Classical phase transition

$$\nu_t^{(c)2} = 2 \left(\frac{2Q^2}{ma^3} \right) \sum_{j=1}^N \frac{1}{j^3} \sin^2 \frac{j\pi}{2}$$

linear

zigzag



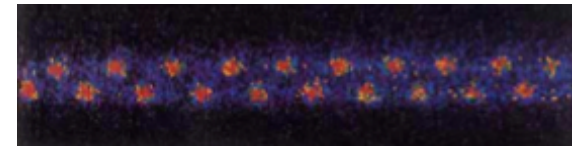
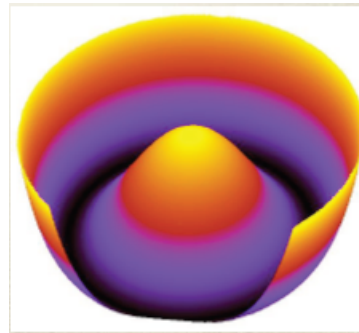
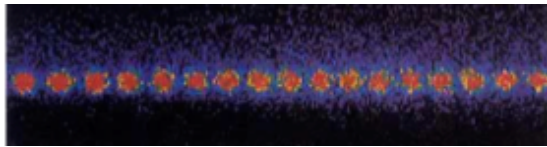
Quantum phase transition

$$\nu_t^{(c)2} = 2 \left(\frac{2Q^2}{ma^3} \right) \sum_{j=1}^N \frac{1}{j^3} \sin^2 \frac{j\pi}{2}$$

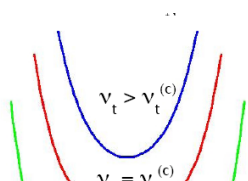
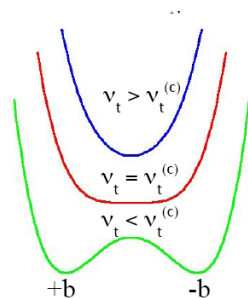
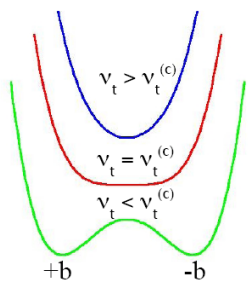
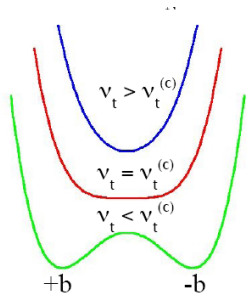
linear

Tunneling: disorder

zigzag



Quantum fluctuations at the mechanical instability (2D)



Soft mode: $y_j^{\text{soft}} = (-1)^j y_0$

Modes close to the instability:

$$y_j = (-1)^j a \phi_j$$

Effective potential:

$$V[\{\phi_j\}] \approx \sum_{j=1}^N V_0(\phi_j) + \frac{1}{2} K \sum_{j=1}^N (\phi_j - \phi_{j+1})^2$$

$$V_0(\phi) = -\frac{1}{2} m(\nu_c^2 - \nu_t^2) a^2 \phi^2 + \frac{1}{4} g a^4 \phi^4$$

Mapping to an Ising model in the transverse field

$$\phi_j = \phi_0 \sigma_j^z + \delta\phi_j$$

$Z \approx Z_0 \int \mathcal{D}\sigma \exp(-S_I[\sigma]/\hbar)$ action of an Ising model

Effective Hamiltonian

$$H_I = - \sum_{j=1}^N (J \sigma_j^z \sigma_{j+1}^z + h \sigma_j^x)$$

$h \approx C_h (U_P U_K^2)^{1/3}$ transverse field (tunneling)

$J = K \phi_0^2 = C_J U_P \epsilon$ exchange coupling (Coulomb interaction)

DMRG results

$$\tilde{H} = \frac{1}{2} \sum_{i=1}^L [\tilde{p}_i^2 + (\tilde{\omega}^2 - \mathcal{M}_1) \tilde{y}_i^2 + \mathcal{M}_2 (\tilde{y}_i + \tilde{y}_{i+1})^2 + \mathcal{M}_3 \tilde{y}_i^4]$$

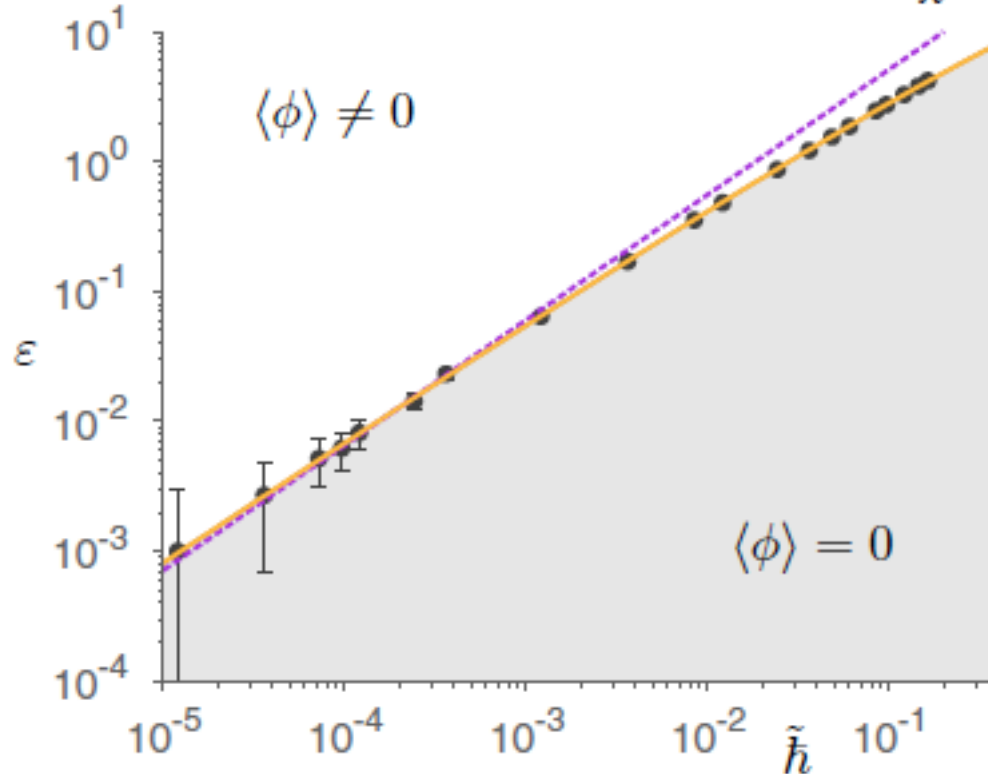
	<i>Quantity</i>	<i>Computed</i>	<i>Theory [11]</i>
η	Anomalous dimension	0.258 ± 0.012	0.25
β	Spont. magnetization	0.126 ± 0.011	0.125
ν	Correlation length	1.03 ± 0.05	1
c	Central charge	0.487 ± 0.015	0.5

Theory: critical exponents of Ising model with transverse field

Quantum effects

shift from the critical point

$$\varepsilon_c \sim \frac{3g\tilde{\hbar}}{\pi} (|\ln \tilde{\hbar}| - |\ln \tilde{\hbar}^*|)$$



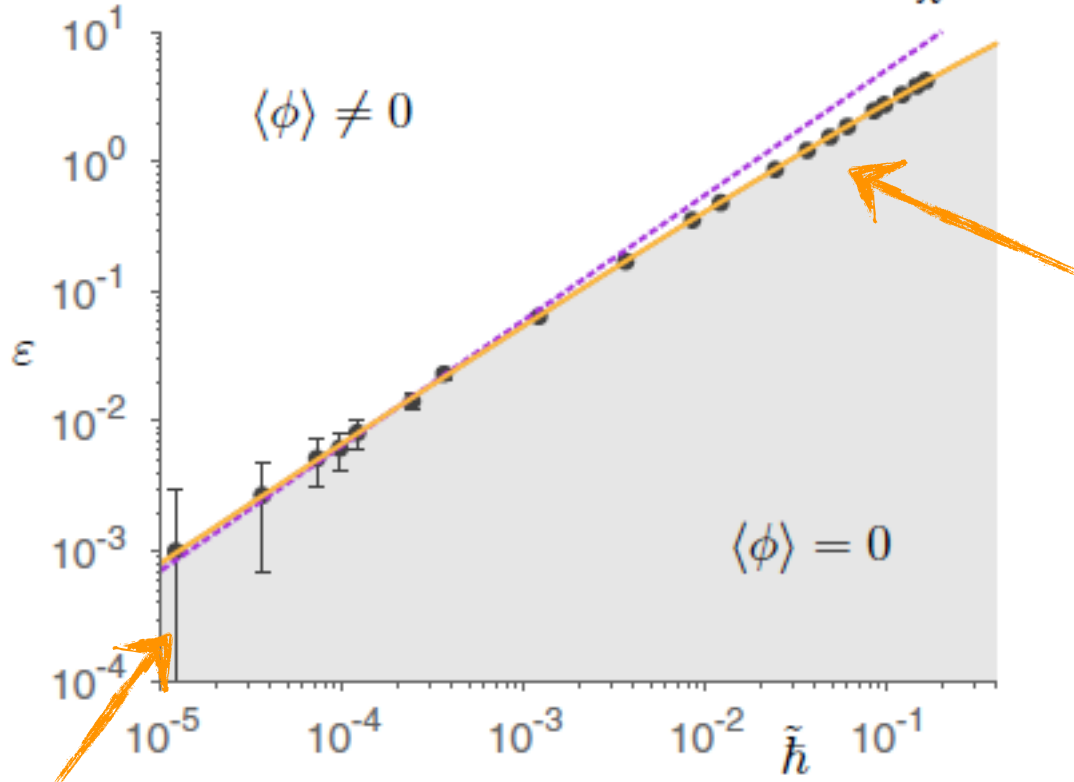
rescaled quantum fluctuations

DMRG and RG flow analysis are in excellent agreement

Quantum effects

shift from the critical point

$$\varepsilon_c \sim \frac{3g\tilde{\hbar}}{\pi} (|\ln \tilde{\hbar}| - |\ln \tilde{\hbar}^*|)$$



dipoles

rescaled quantum fluctuations

ions:

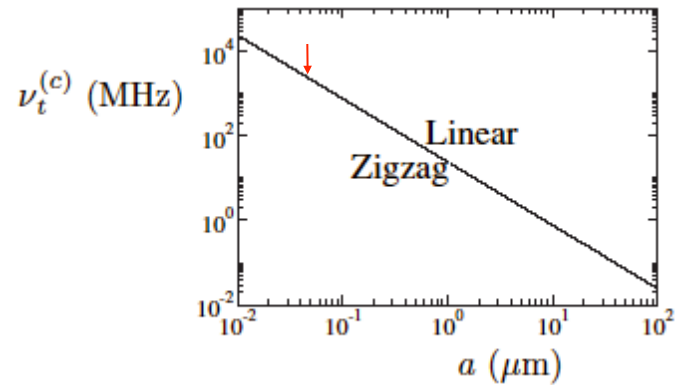
quantum effects are negligible

Dynamics:

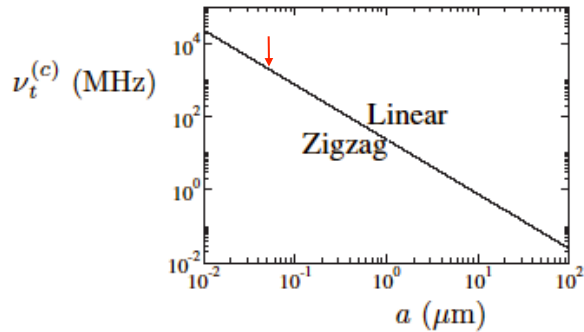
**classical and quantum
quenches**

Classical quenches
at the linear-zigzag instability

Preamble: scaling at the classical phase transition

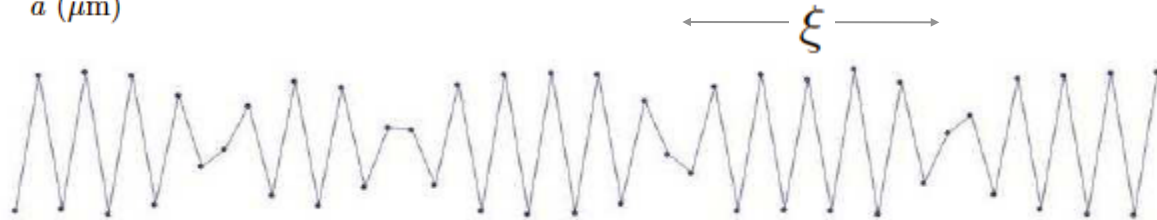


Preamble: scaling at the classical phase transition

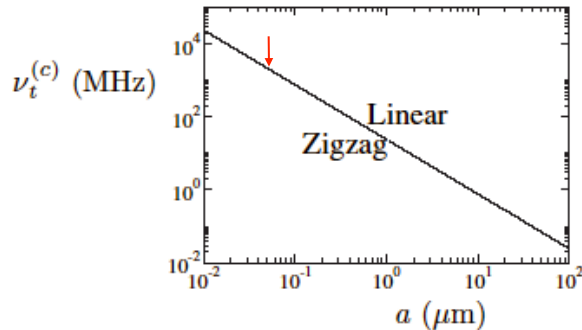


Correlation length (Landau)

$$\xi \sim (\nu_t - \nu_t^{(c)})^{-1/2}$$

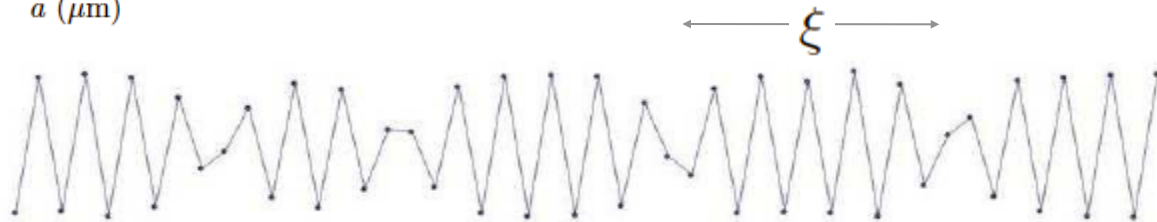


Preamble: scaling at the classical phase transition



Correlation length (Landau)

$$\xi \sim (\nu_t - \nu_t^{(c)})^{-1/2}$$

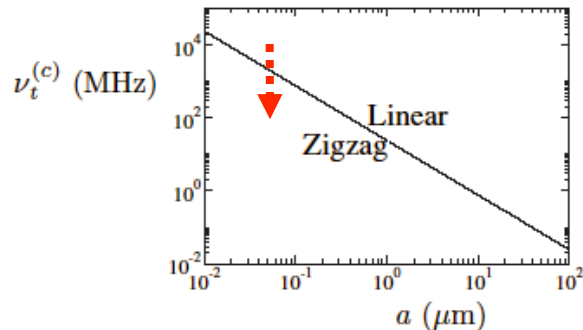


Relaxation time (Landau)

$$\tau \sim (\nu_t - \nu_t^{(c)})^{-1}$$

it diverges at the critical point

Dynamical properties at criticality



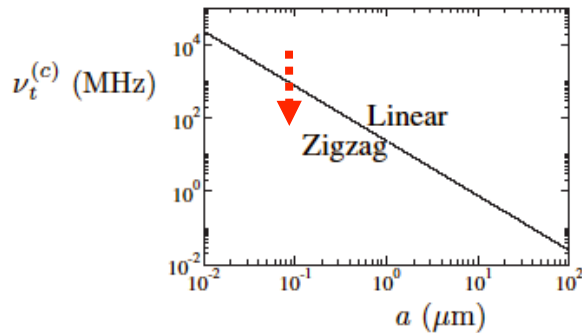
$$\nu_t = \sqrt{\nu_t^{(c)2} + \delta(t)}$$

$$\delta(t) = -\delta_0 \frac{t}{\tau_Q}$$

Dynamics of the order parameter:
Landau Ginzburg equation in presence of damping
(laser cooling)

$$\partial_t^2 \psi - h(x)^2 \partial_x^2 \psi + \eta \partial_t \psi + \delta(x, t) \psi + 2\mathcal{A}(x) \psi^3 = \varepsilon(t)$$

Kibble-Zurek mechanism



$$\partial_t^2 \psi - h(x)^2 \partial_x^2 \psi + \eta \partial_t \psi + \delta(x, t) \psi + 2\mathcal{A}(x) \psi^3 = \varepsilon(t)$$

$$\nu_t = \sqrt{\nu_t^{(c)2} + \delta(t)}$$

$$\delta(t) = -\delta_0 \frac{t}{\tau_Q}$$

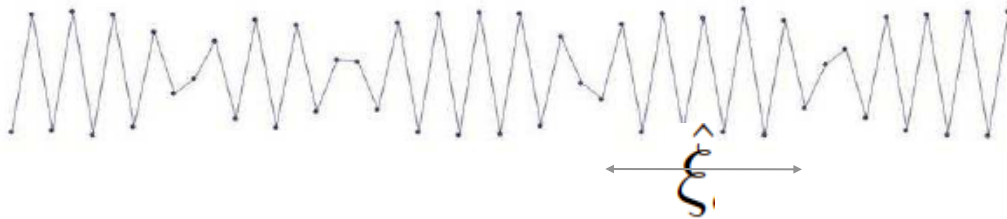
Kibble-Zurek hypothesis: $\tau \sim (\nu_t - \nu_t^{(c)})^{-1}$

System follows the quench adiabatically till the relaxation time becomes slower than the quench.

Freeze-out time: $\tau(\hat{t}) = \hat{t}$ Density of defects: $d_o \sim \frac{1}{\hat{\xi}_o}$

Density of defects after the quench

Scaling of the density of defects as a function of the quench rate:



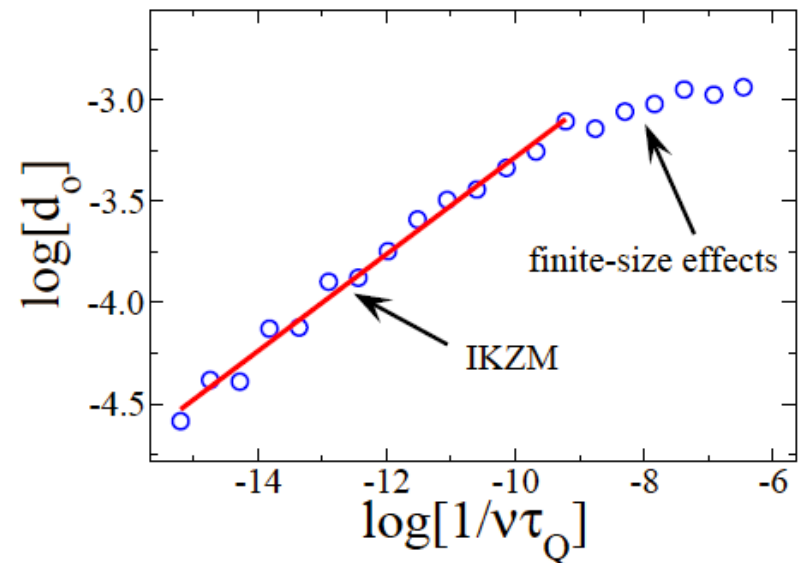
overdamped case:

$$d_o \sim \frac{2\hat{X}_*}{\hat{\xi}} \sim \frac{L}{3\nu_l^{(c)}(0)^2 a^2 \omega_0^2} \frac{\eta \delta_0}{\tau_Q}$$

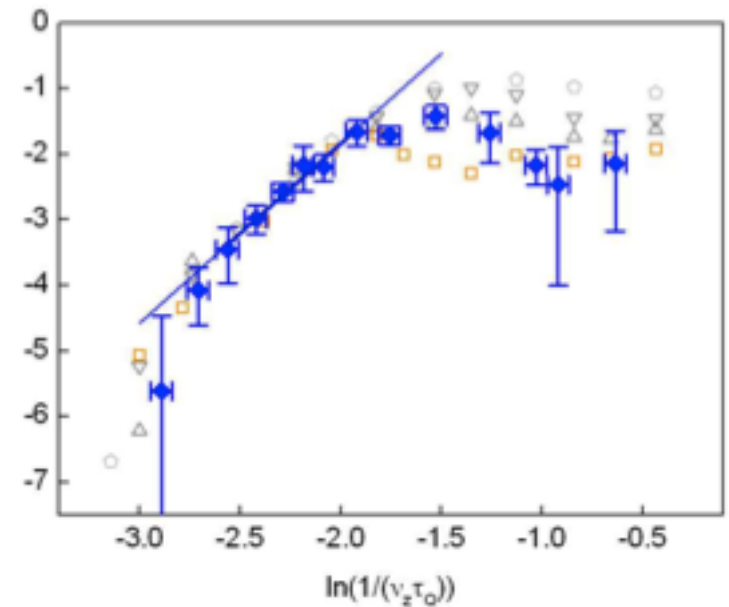
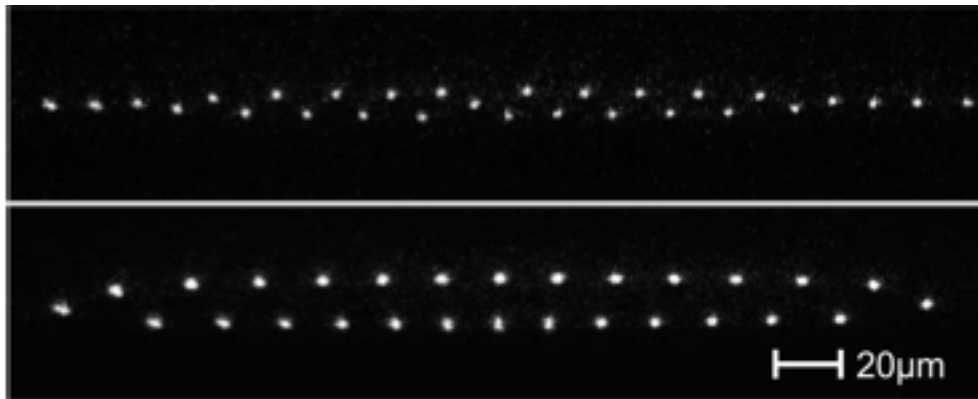
underdamped case:

$$d_u \sim \frac{2\hat{X}_*}{\hat{\xi}} = \frac{L}{3\nu_l^{(c)}(0)^2 a^2 \omega_0^2} \left(\frac{\delta_0}{\tau_Q}\right)^{4/3}$$

[Laguna and Zurek, PRL 1999]



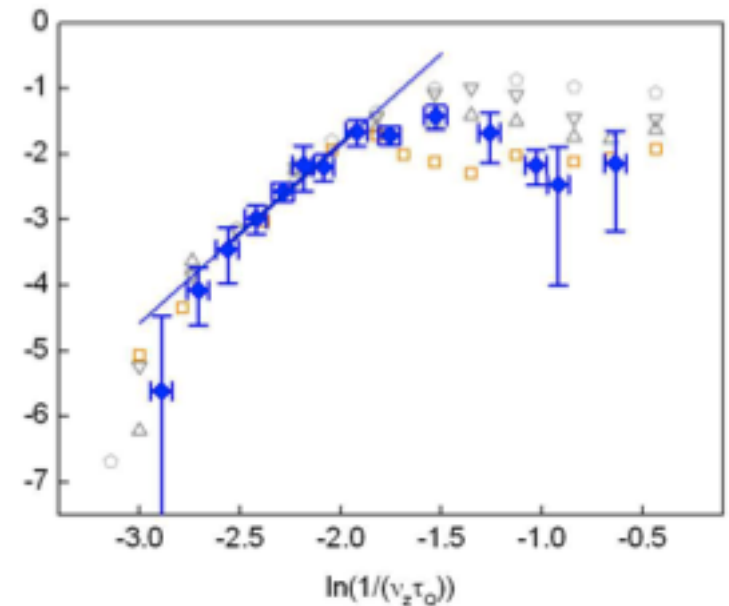
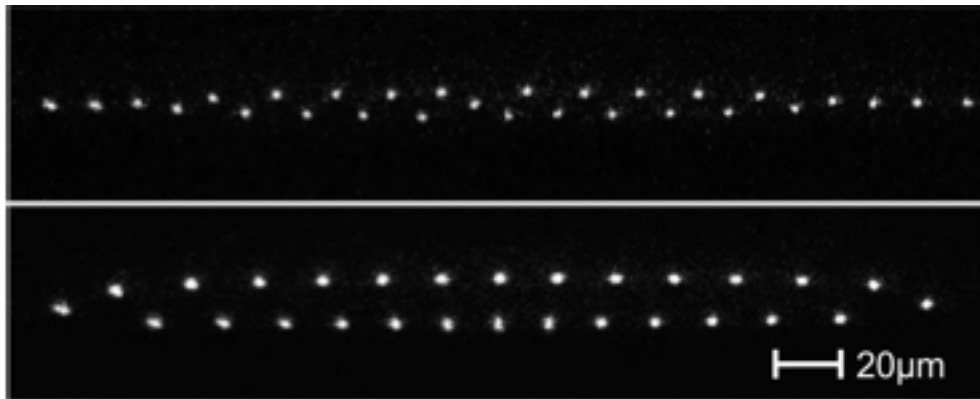
Experimental quenches



T. Mehlstäubler and coworkers (PTB)

See also: Schätz (Freiburg) and Schmidt-Kaler (Mainz)

Experimental quenches



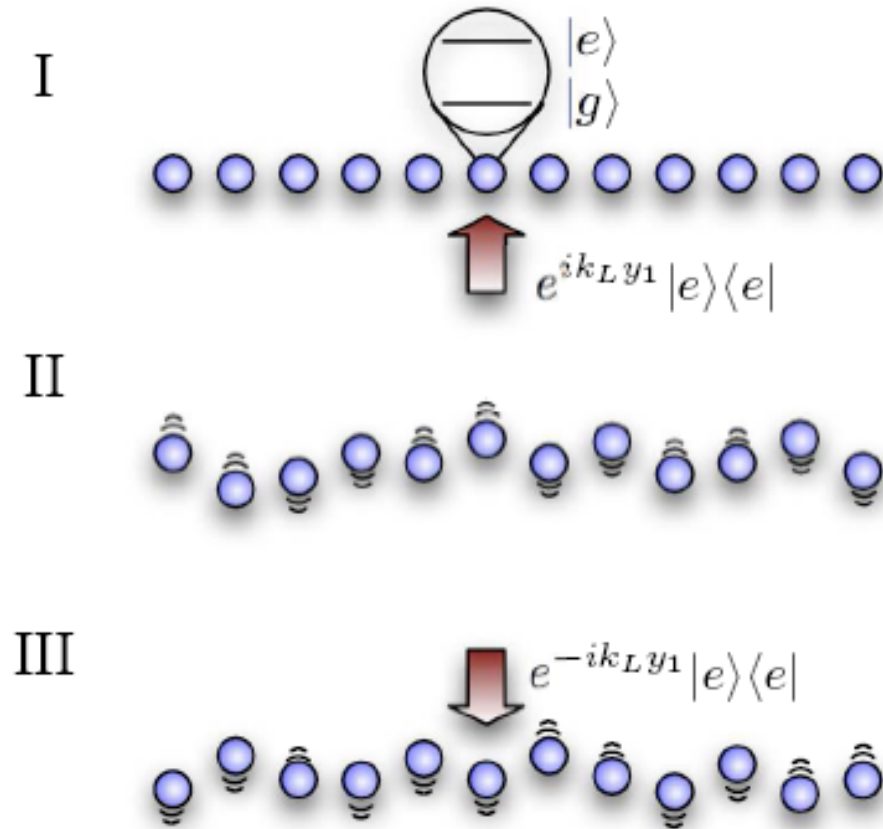
T. Mehlstäubler and coworkers (PTB)

What's next: spectroscopy and control of the kinks

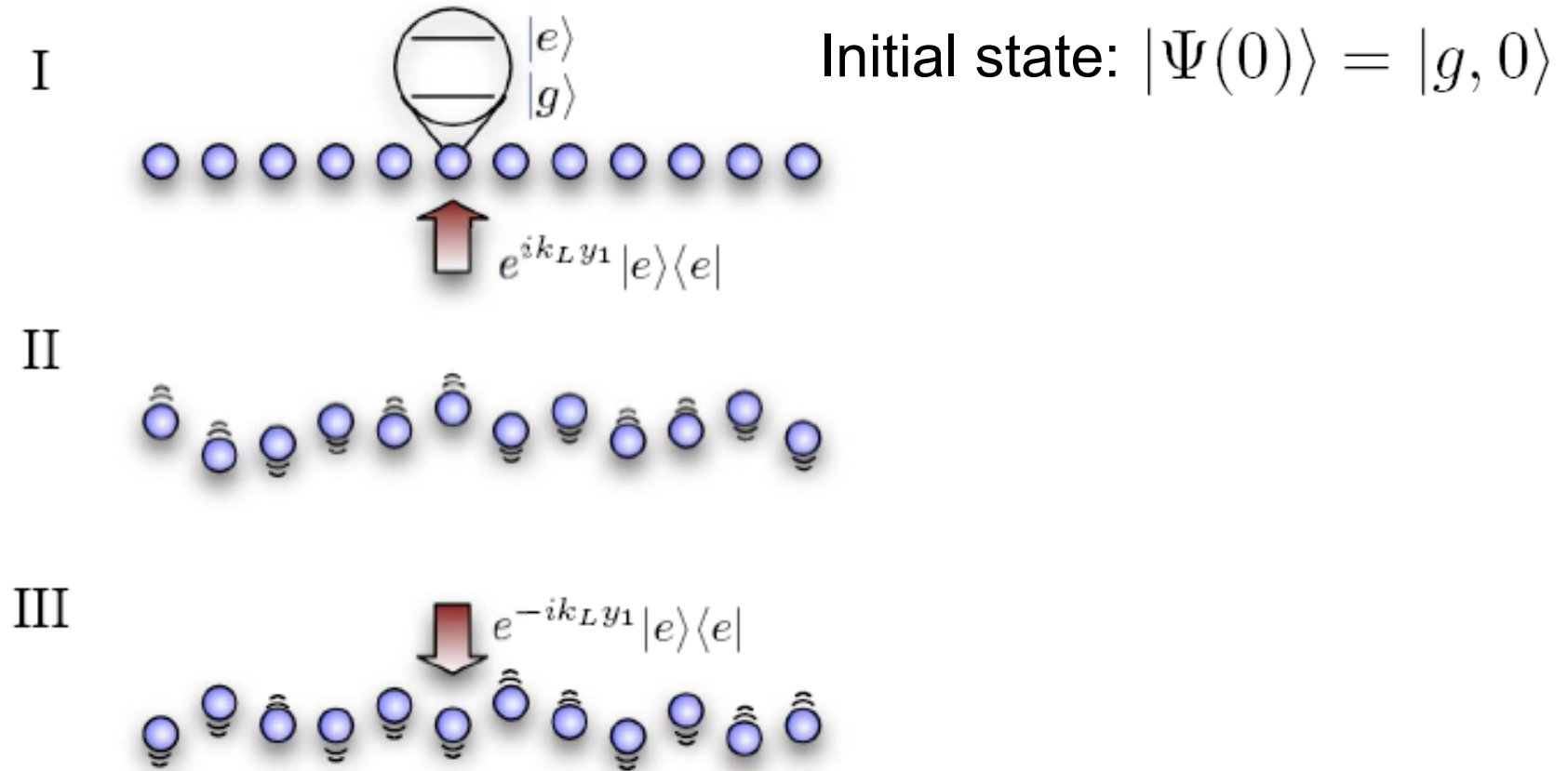
See also: Schätz (Freiburg) and Schmidt-Kaler (Mainz)

Sudden quenches in a linear chain

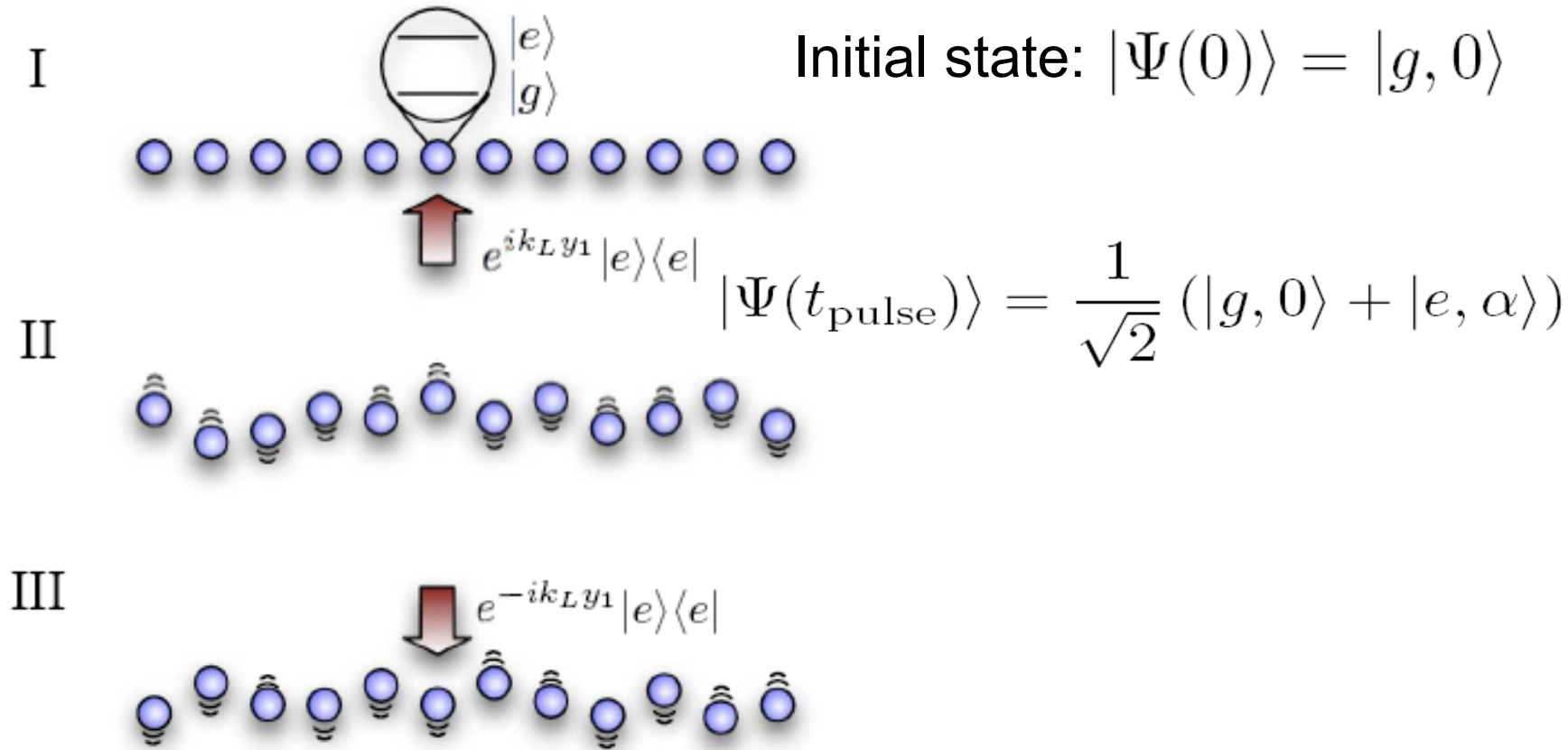
Ramsey interferometry



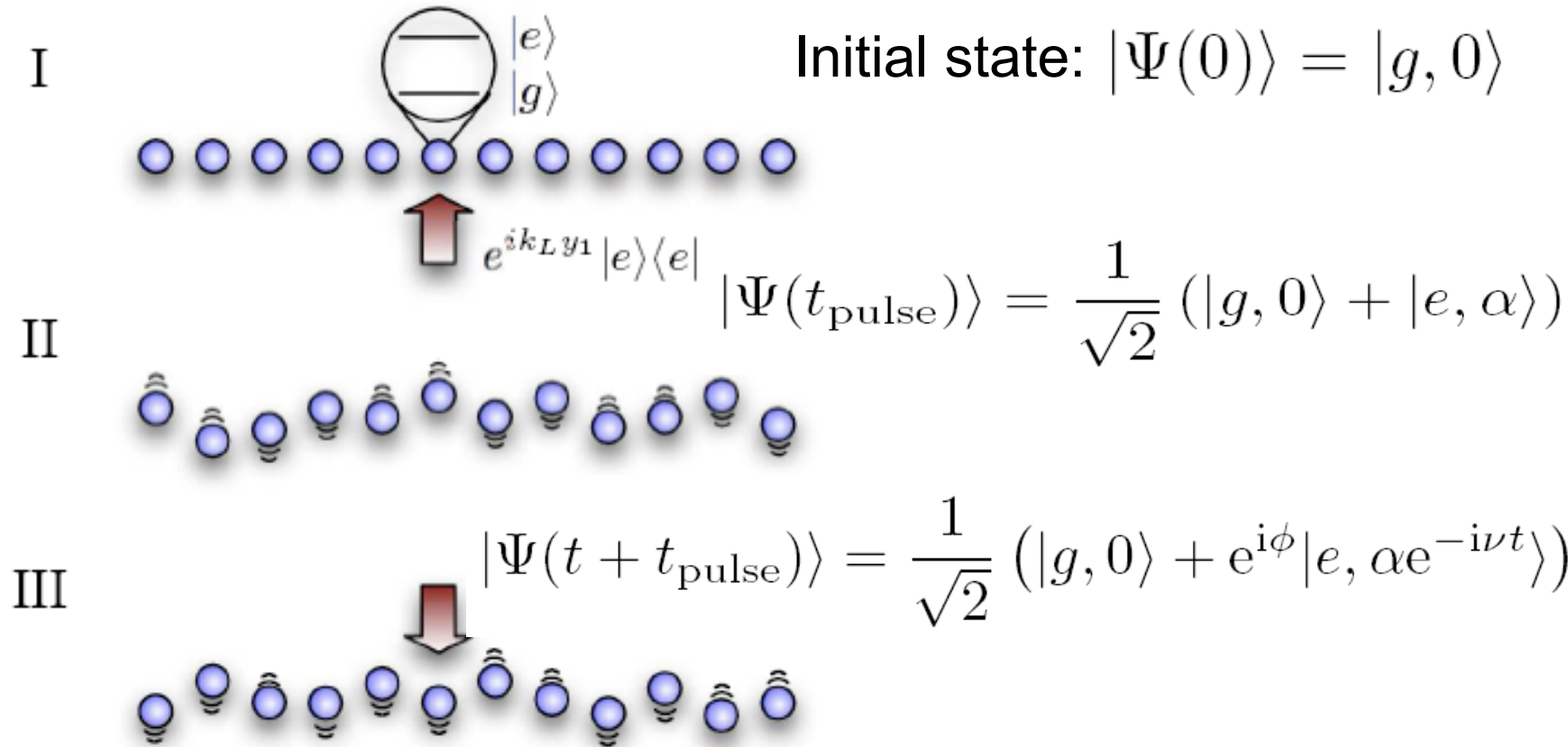
Ramsey interferometry



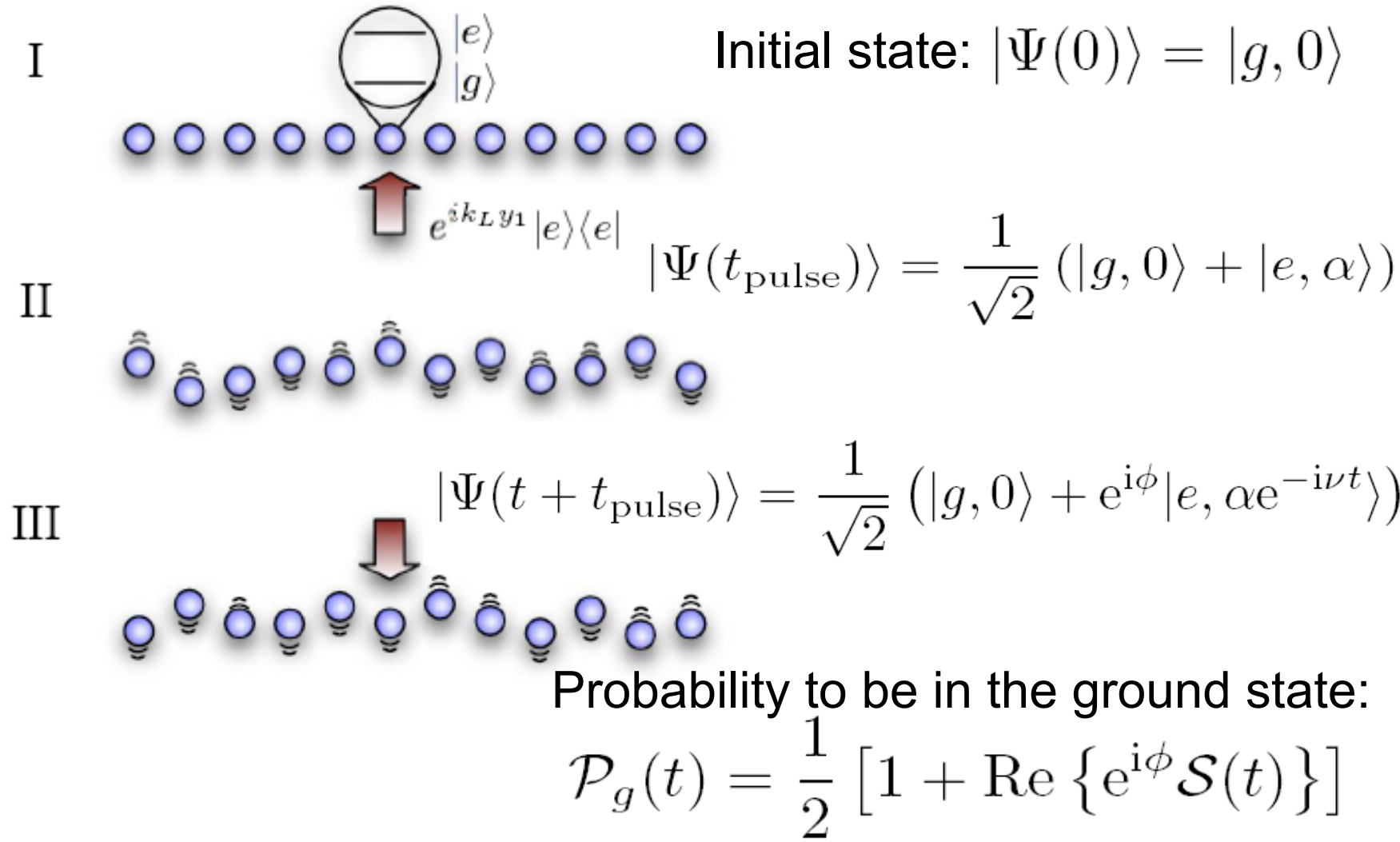
Ramsey interferometry



Ramsey interferometry



Ramsey interferometry



Cat-states in spin-dependent potentials

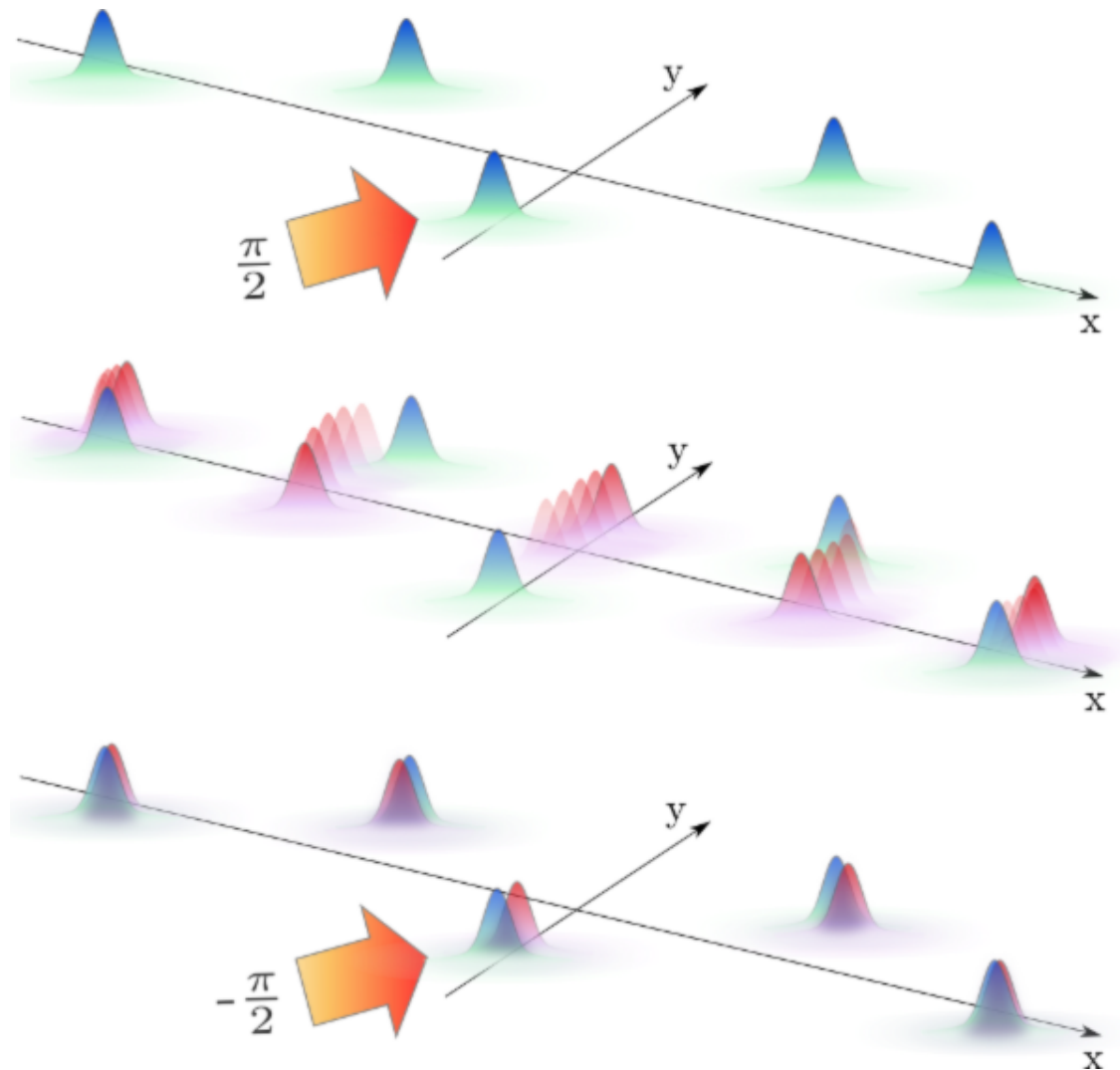
Quantum superposition of two internal states
in a spin-dependent potential

$$V_{\text{pot}} = \sum_{j=1}^N |g\rangle_j \langle g| V_g(\mathbf{r}_j) + |e\rangle_j \langle e| V_e(\mathbf{r}_j)$$

Cat-state of ion structures

$$|\Psi(t)\rangle = \frac{1}{\sqrt{2}} \left(|ggg\rangle |0\rangle_{zz} + |geg\rangle |\phi(t)\rangle \right)$$

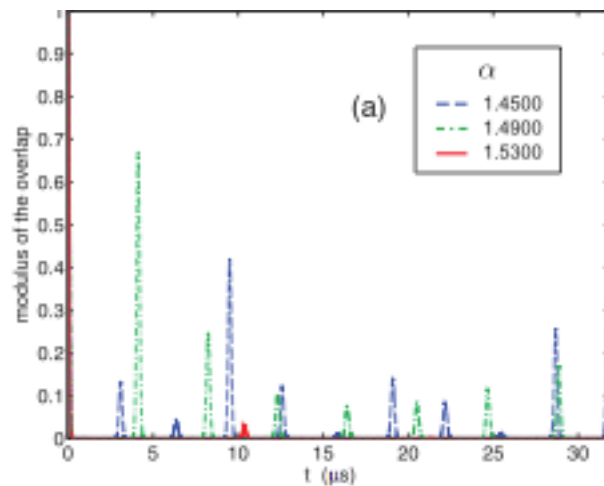
Cat-states in spin-dependent potentials



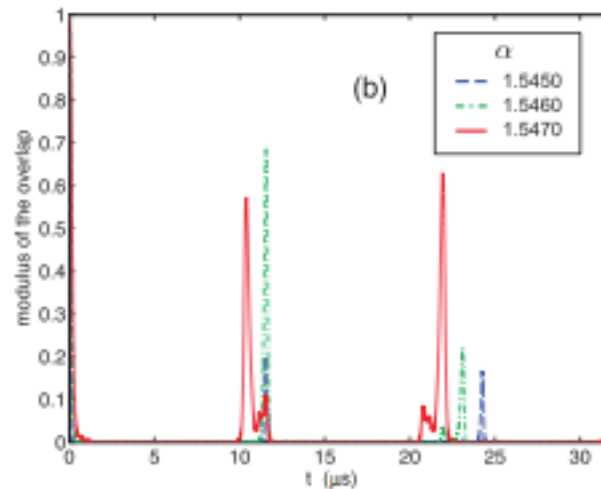
Ramsey contrast

Ramsey contrast gives the overlap between the two motional states across the transition

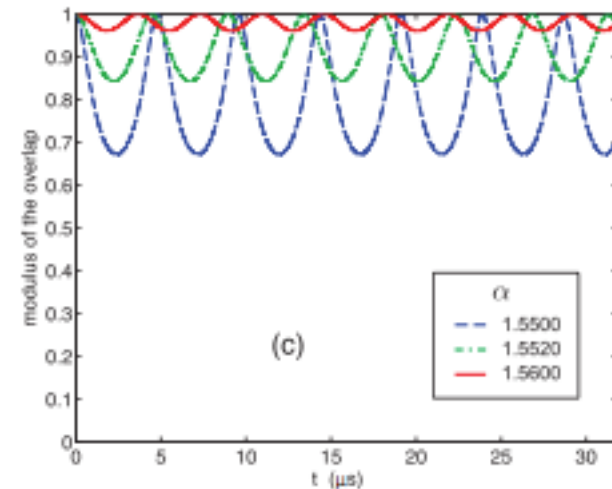
zigzag-zigzag



zigzag-linear



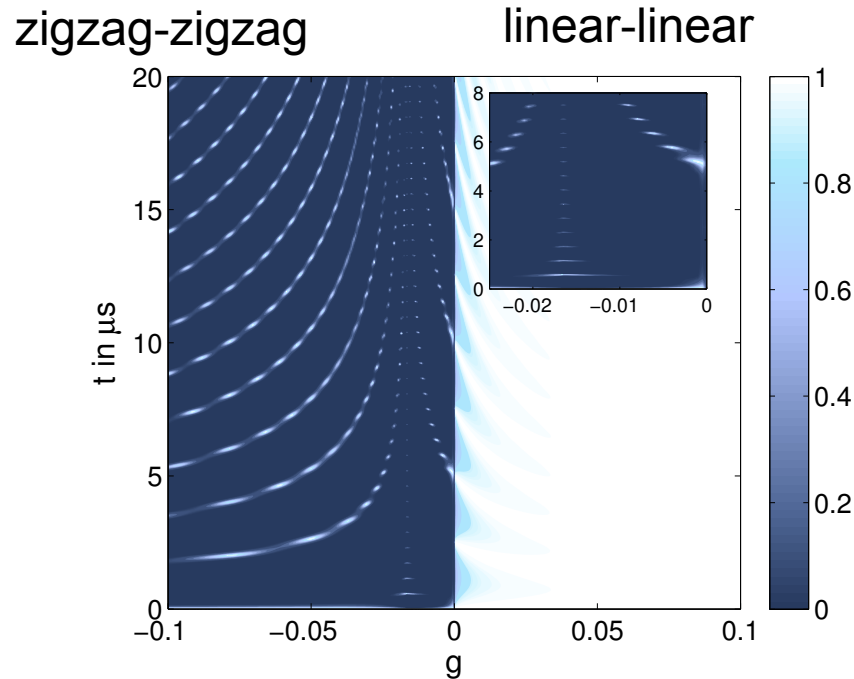
linear-linear



Visibility signal

Visibility gives the overlap of the states across the quench

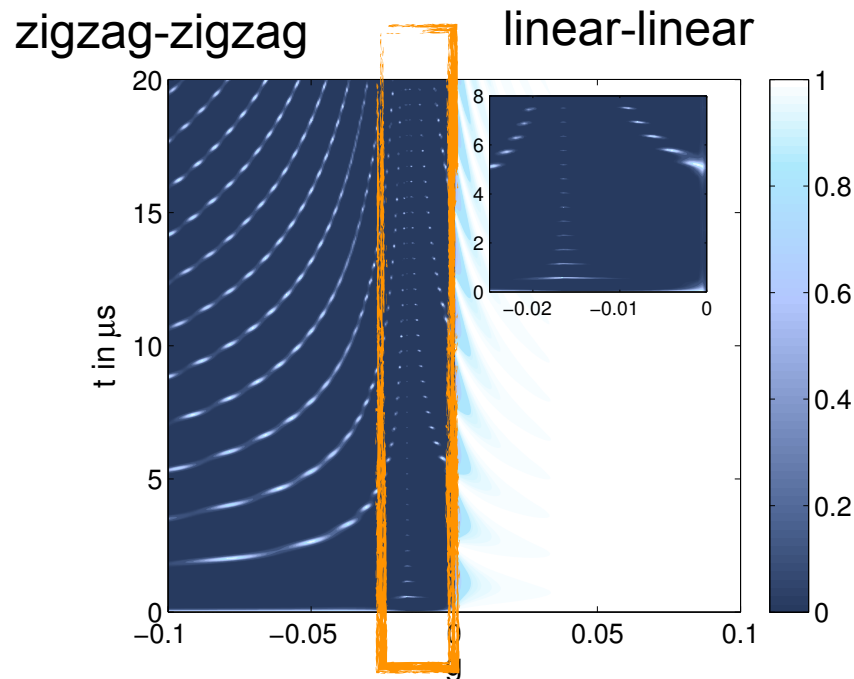
$$\mathcal{O}_0(t) = {}_g\langle \underline{0} | U_e(t) | \underline{0} \rangle_g$$



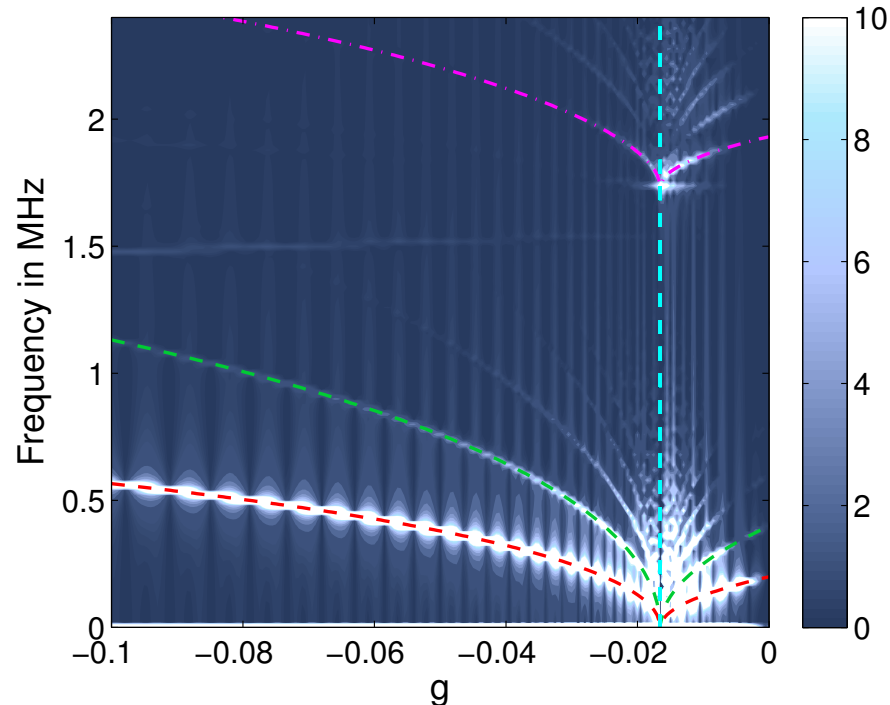
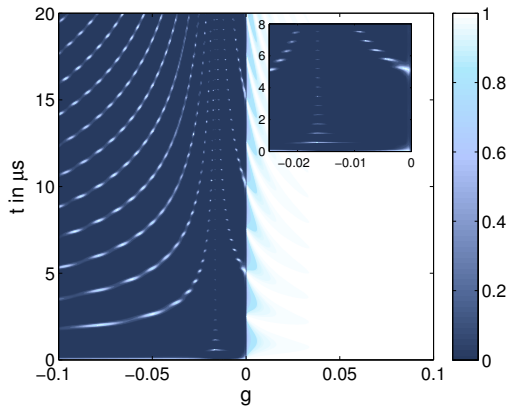
Visibility signal

Visibility gives the overlap of the states across the quench

$$\mathcal{O}_0(t) = {}_g\langle \underline{0} | U_e(t) | \underline{0} \rangle_g$$

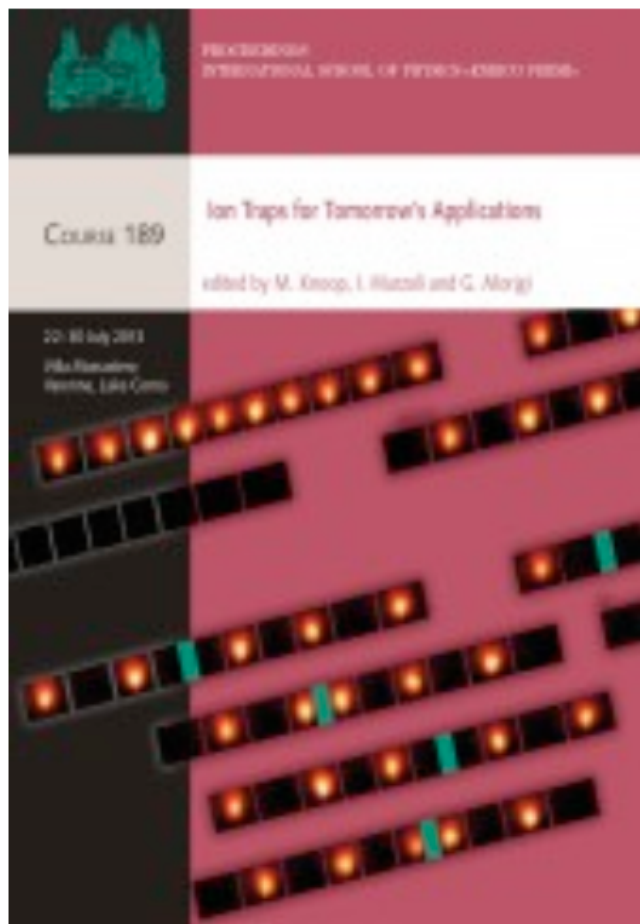


Fourier transform of the Visibility signal



Revivals at the frequency of the soft mode:
independent of the size
signature of macroscopic quantum coherence

Quantum Quenches



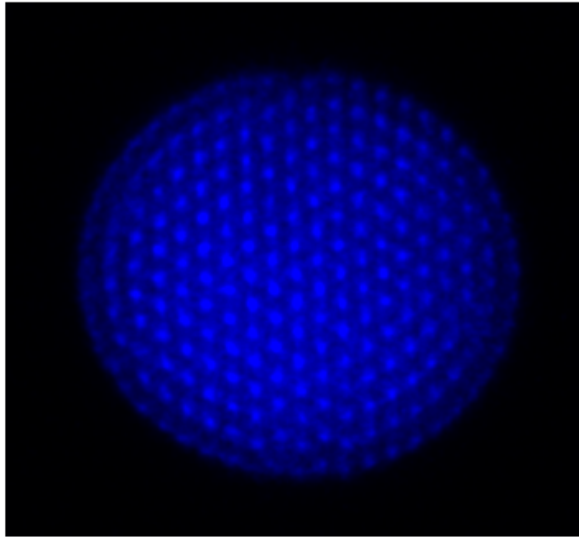
Based on engineering the coupling between phonons and spins (Wunderlich, Porras, Cirac)

Experiments:
Blatt, Bollinger, Monroe, Schätz,
....

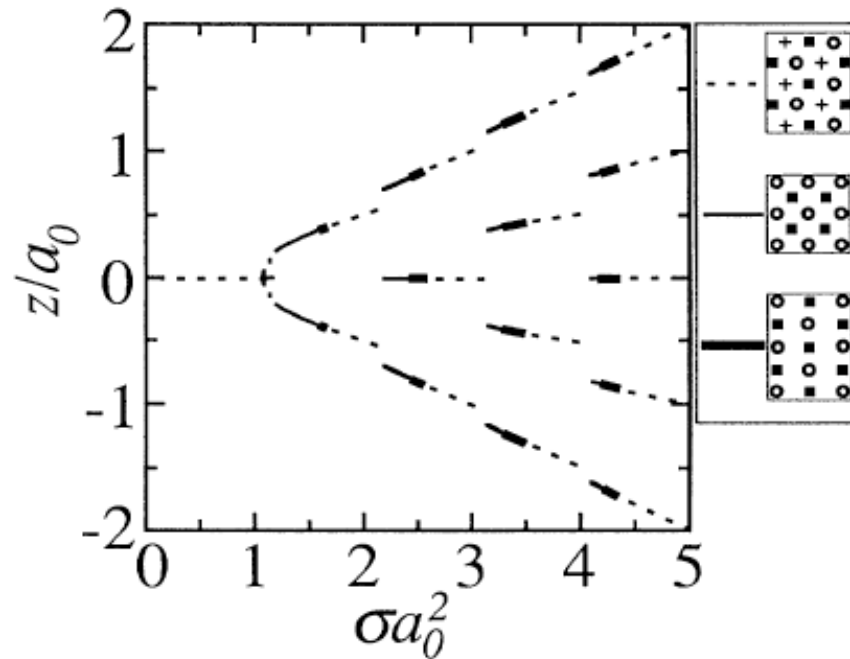
Picture: Chris Monroe's group

Topological Phase Transitions in Ion Crystals

Planar instability



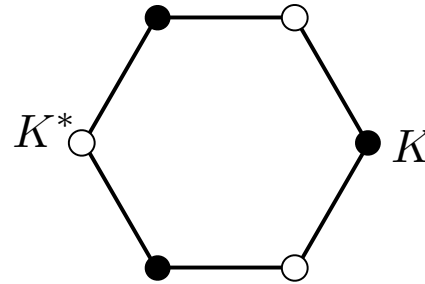
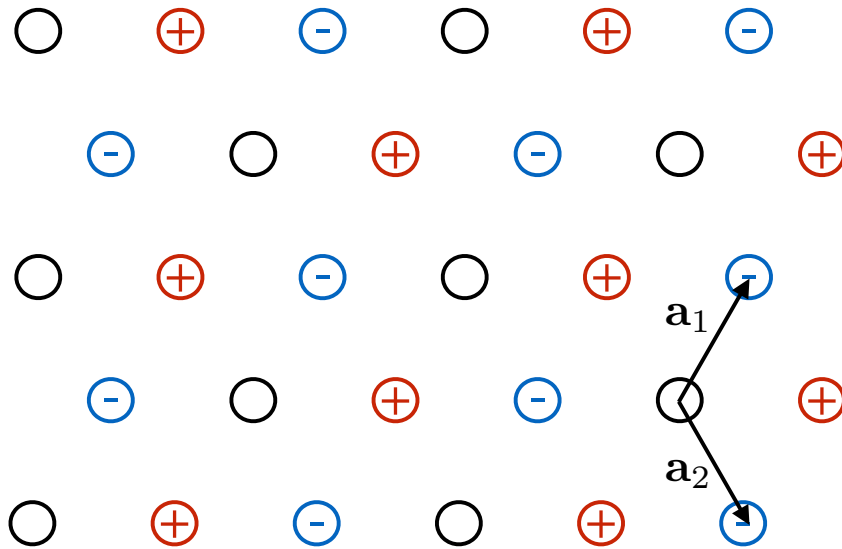
(M. Drewsen & coworkers, Aarhus)



D.H.E. Dubin, PRL 1993

Continuous transition from a single to three planes

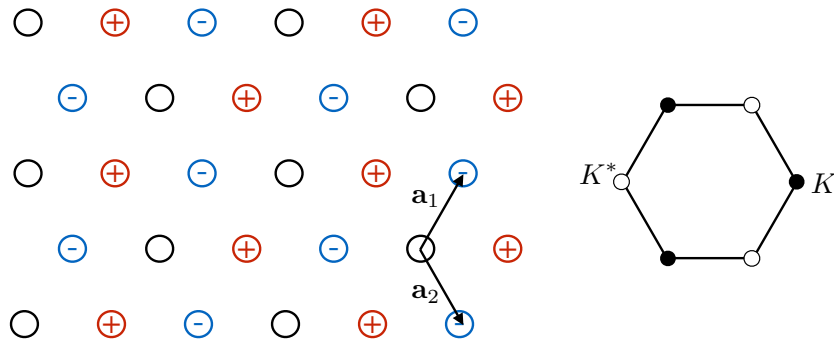
Order parameter



order parameter

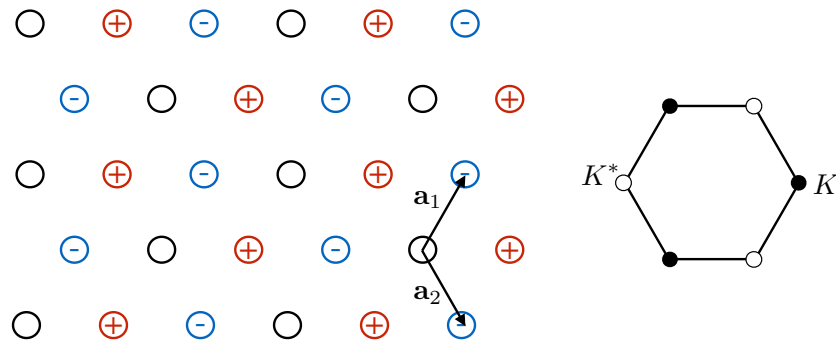
$$z_i = \text{Re} [\psi e^{i\mathbf{K} \cdot \mathbf{r}_i}]$$

Symmetries and Model



$$R_z : \psi \rightarrow -\psi ,$$
$$T_{\mathbf{a}_1} : \psi \rightarrow \psi e^{2\pi i/3} ,$$
$$R_x : \psi \rightarrow \psi^* ,$$

Symmetries and Model



$$R_z : \psi \rightarrow -\psi,$$

$$T_{\mathbf{a}_1} : \psi \rightarrow \psi e^{2\pi i/3},$$

$$R_x : \psi \rightarrow \psi^*,$$

Ginzburg-Landau free energy

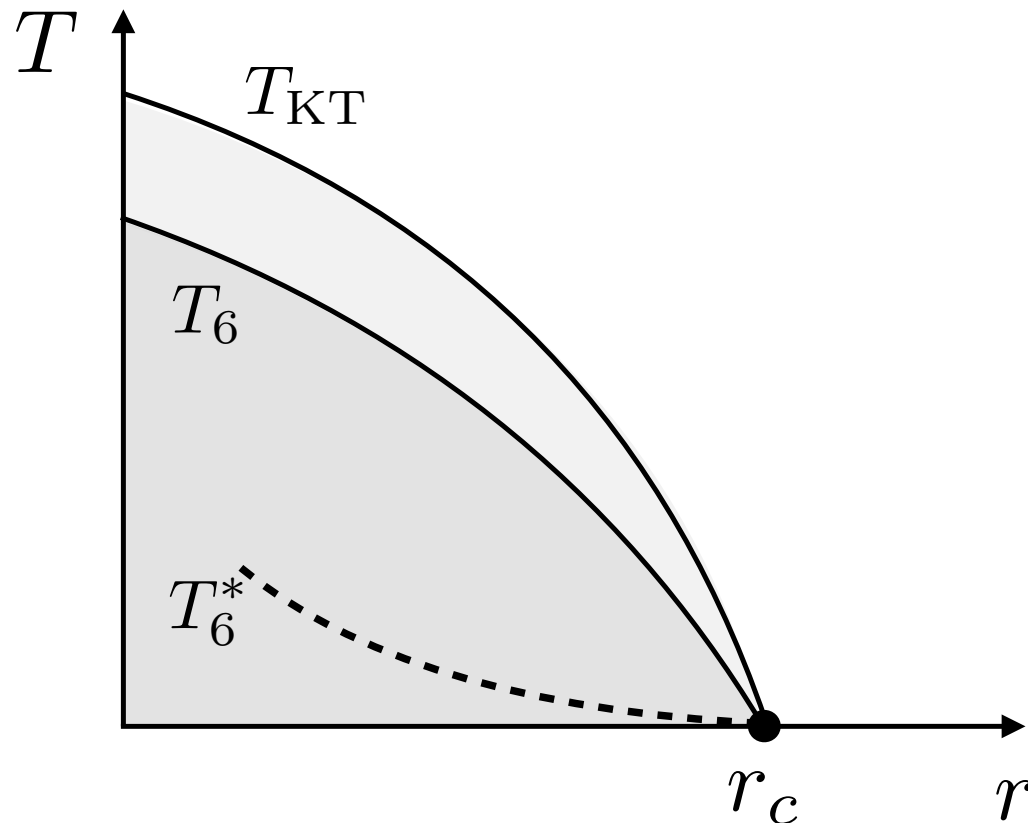
$$\frac{f_{GL}}{\mathcal{K}} = \frac{\gamma}{2} |\nabla \psi|^2 + r|\psi|^2 + u|\psi|^4 + v|\psi|^6 + \frac{w}{2} [\psi^6 + (\psi^*)^6]$$

6-state clock model

Phase diagram

6-state clock model

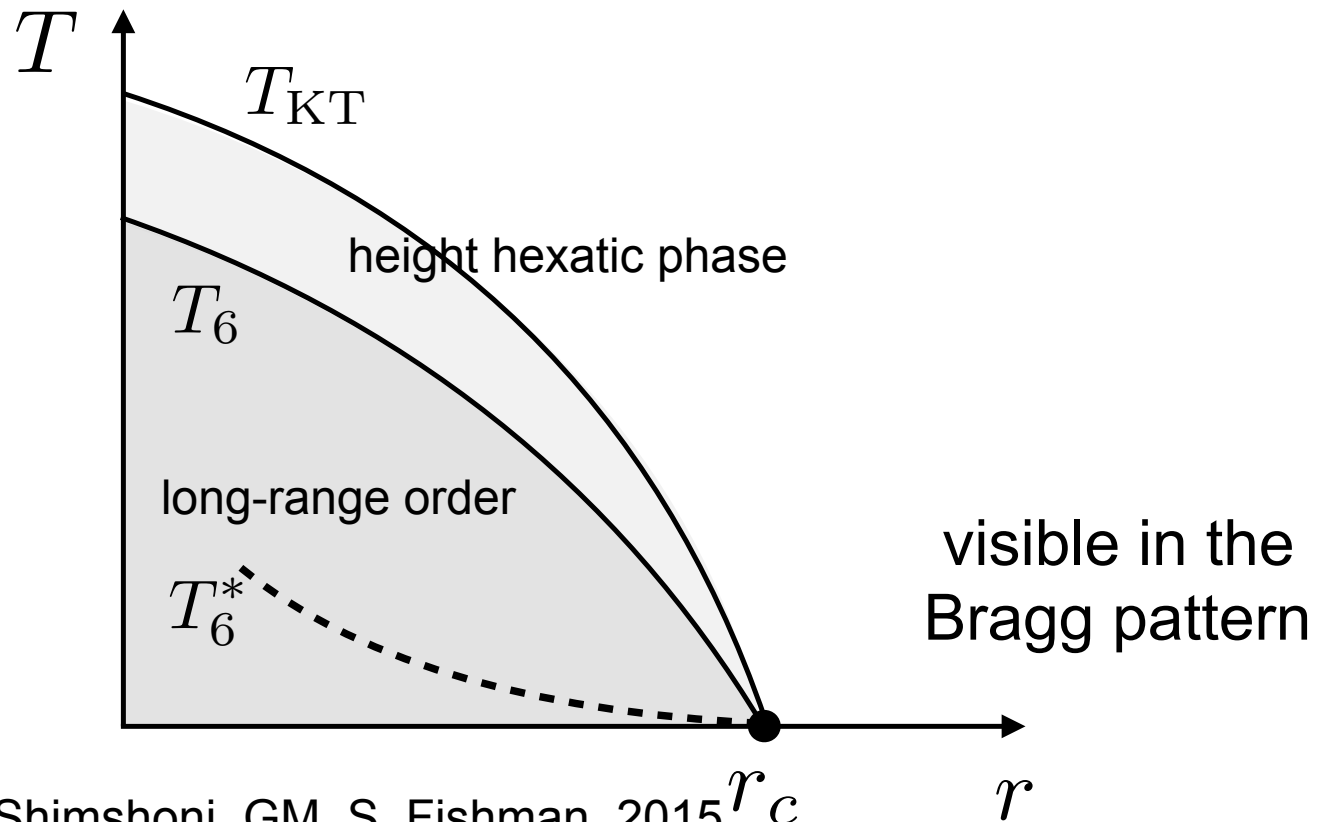
$$\frac{f_{\text{GL}}}{\mathcal{K}} = \frac{\gamma}{2} |\nabla \psi|^2 + r |\psi|^2 + u |\psi|^4 + v |\psi|^6 + \frac{w}{2} [\psi^6 + (\psi^*)^6]$$



Phase diagram

6-state clock model

$$\frac{f_{\text{GL}}}{\mathcal{K}} = \frac{\gamma}{2} |\nabla \psi|^2 + r |\psi|^2 + u |\psi|^4 + v |\psi|^6 + \frac{w}{2} [\psi^6 + (\psi^*)^6]$$



Conclusions

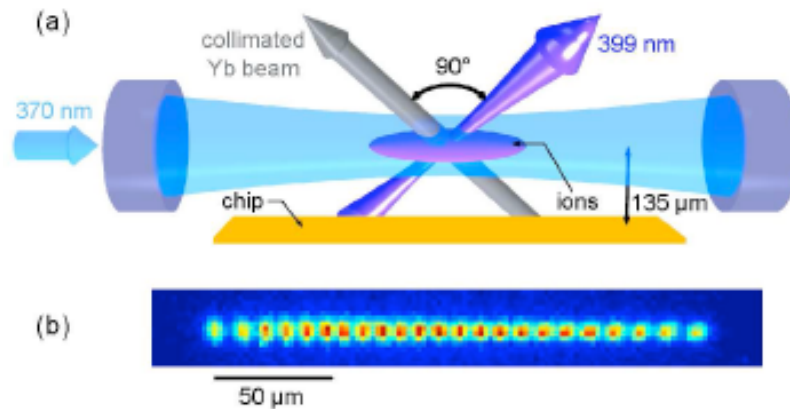
Structural transitions in ion crystals: “natural” quantum simulators of solid-state models

Ion crystals: laboratory for studying far-off equilibrium statistical mechanics

Interfacing phonons and photons: novel quantum phases of matter

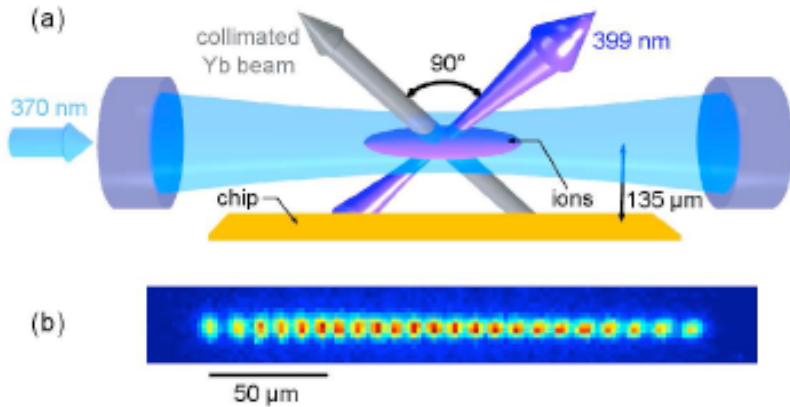
Exotic phases of photons and ions

Ion crystal in a cavity

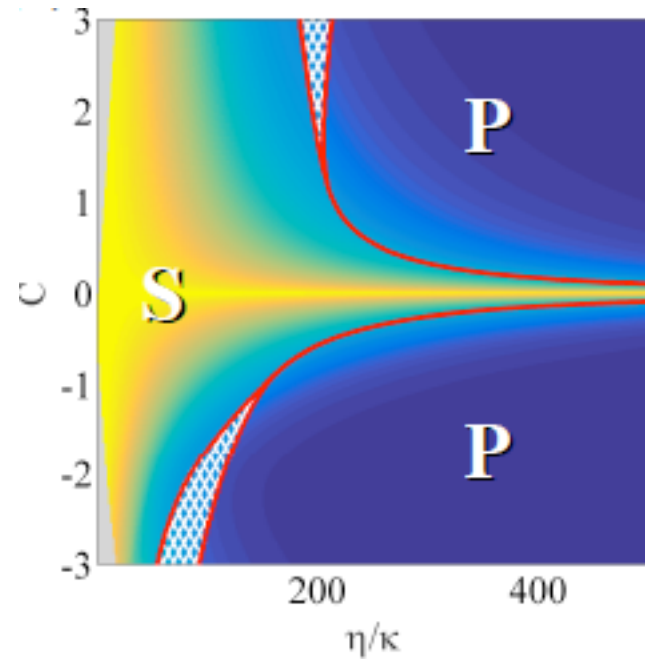


Typical length of crystallization is incommensurate
with cavity wave length
(figure from Cetina et al, NJP 2013)

Exotic phases of photons and ions



Exotic model of friction



Collaborations

Shmuel Fishman and Daniel Podolsky, Technion, Haifa

Efrat Shimshoni, Bar-Ilan, Tel Aviv

Pietro Silvi, Simone Montangero, Tommaso Calarco, Ulm

Alex Retzker, Adolfo del Campo, Martin Plenio, Ulm

Grigory Astrakharchik and Jordi Boronat, UPC Barcelona

Thomas Fogarty and Thomas Busch, Cork



BMBF
QuORep



DFG







J. Baltrusch

G. De Chiara

T. Fogarty

C. Cormick E. Kajari

